Major article

Redistribution of the novel *C. difficile* spore-adherence receptor, E-cadherin, by TcdA and TcdB increases spore-association to adherens junctions.

Pablo Castro-Córdova[1,#,$], Macarena Otto-Medina[2,#], Nicolás Montes-Bravo[1,#], Christian Brito-Silva[1], D. Borden Lacy[3], Daniel Paredes-Sabja [1,4]*

[#] Authors contributed equally to this work.

[1] ANID – Millennium Science Initiative Program – Millennium Nucleus in the Biology of the Intestinal Microbiota, Santiago, Chile.

[2].Departamento de Ciencias Biológicas, Facultad de Ciencias de la Vida, Universidad Andrés Bello, Santiago, Chile.

[3] Department of Pathology, Microbiology, and Immunology, Vanderbilt University School of Medicine, Nashville, Tennessee, USA.

[4] Department of Biology, Texas A&M University, College Station, Texas, USA.

[$]Present address: Laboratory of Nano-Regenerative Medicine, Centro de Investigación e Innovación Biomédica (CiiB), Universidad de los Andes, Santiago, Chile

Short Title: Association of *C. difficile* spores to adherens junctions.

Key Words:

C. difficile spores, E-cadherin, spore-host interaction, *C. difficile* toxins TcdA/TcdB.

24 *Corresponding Author. Dr. Daniel Paredes-Sabja, Department of Biology, Texas A&M
25 University, College Station, TX, 77843, USA. E-mail: dparedes-sabja@bio.tamu.edu
26

ABSTRACT

Clostridioides difficile causes antibiotic-associated diseases in humans ranging from mild diarrhea to severe pseudomembranous colitis and death. A major clinical challenge is the prevention of disease recurrence, which affects nearly ~20 – 30 % of the patients with a primary *C. difficile* infection (CDI). During CDI, *C. difficile* forms metabolically dormant spores that are essential for recurrence of CDI (R-CDI). In prior studies, we have shown that *C. difficile* spores interact with intestinal epithelial cells (IECs), which contributes to R-CDI. However, this interaction remains poorly understood. Here, we provide evidence that *C. difficile* spores interact with E-cadherin, contributing to spore-adherence and internalization into IECs. *C. difficile* toxins TcdA/TcdB lead to adherens junctions opening and increase spore-adherence to IECs. Confocal micrographs demonstrate that *C. difficile* spores associate with accessible E-cadherin; spore-E-cadherin association increases upon TcdA/TcdB intoxication. The presence of anti-E-cadherin antibodies decreased spore adherence and entry into IECs. By ELISA, immunofluorescence, and immunogold labelling, we observed that E-cadherin binds to *C. difficile* spores, specifically to the hair-like projections of the spore, reducing spore-adherence to IECs. Overall, these results expand our knowledge of how *C. difficile* spores bind to IECs by providing evidence that E-cadherin acts as a spore-adherence receptor to IECs and by revealing how toxin-mediated damage affects spore interactions with IECs.

46 **INTRODUCTION**

47 *C. difficile* is a Gram-positive, anaerobic, spore-forming bacterium and the main causative
48 agent of antibiotic-associated diarrhea, causing death in ~5% of cases (1, 2). R-CDI is a major
49 clinical challenge affecting ~30% of CDI patients (2, 3). CDI is primarily driven by the *C. difficile*
50 toxins TcdA and TcdB, with contributions from the binary transferase toxin in some cases (4-6).
51 Both TcdA and TcdB target their intracellular glucosyltransferase activity towards RhoA, Rac1,
52 and Cdc42 (7, 8). This inhibitory modification of the Rho GTPase family leads to actin
53 depolymerization and disruption of tight and adherens junctions (9-13), causing disruption of
54 epithelial paracellular barrier function (14). Clinical studies showed that administration of anti-
55 TcdB antibody (bezlotoxumab) in combination with antibiotics reduces R-CDI rates (15). The
56 antibody may prevent toxin-mediated stem cell dysfunction and therefore prevent the delay in
57 recovery and repair of the intestinal epithelium (10).

58

59 During infection, *C. difficile* produces spores (16). Strains unable to form spores do not
60 cause R-CDI in animal models (17), indicating that the spores are critical for R-CDI. EDTA-
61 disruption of cell-cell junctions in Caco-2 cells leads to increased adherence of *C. difficile* spores
62 at the cell-cell junction, suggesting a tropism for cell-cell junctions (18). *C. difficile* spores bind to
63 fibronectin and vitronectin, located in the basolateral membrane (19). These molecules contribute
64 to *C. difficile* spore internalization into IECs in an integrin-dependent manner, and spore-entry *in*
65 *vivo* contributes to the R-CDI (20).

66

67 The intestinal barrier is an impermeable layer that separates the apical and basolateral cell
68 sides (21), and is formed by junctions between adjacent IECs. The cell-cell junctions between IECs

69 are constituted of E-cadherin containing adherens junctions and tight junctions formed by claudins,
70 occludins, and zonula occludens. These junctions provide the gut barrier with impermeability
71 properties and restrict the translocation of pathogens and commensal bacteria. However, some
72 pathogens can alter or disrupt the cell junctions, to translocate through the host (22).
73
74 Several enteric pathogens such as *Streptococcus pneumoniae*, *Fusobacterium nucleatum*,
75 *Campylobacter jejuni*, and *Listeria monocytogenes* take advantage of disrupted intestinal adherens
76 junctions to internalize in host cells (23-27). How *C. difficile* spores interact with adherens
77 junctions remains poorly described. Herein, we show that accessible E-cadherin is reduced in
78 differentiated Caco-2 cells. Also, TcdA/TcdB intoxication increases the spore adherence that is
79 correlated with an increase in E-cadherin accessibility in IECs. Next, we observed that *C. difficile*
80 spores interact with E-cadherin in healthy IECs and the binding is increased in TcdA/TcdB-
81 intoxicated cells. Also, the blocking of the cellular E-cadherin with monoclonal antibodies reduces
82 the spore adherence and entry to IECs. Finally, we observed that E-cadherin binds to the hair-like
83 extensions of the exosporium.
84
85 **METHODS**
86 **Bacterial growth conditions.**
87 *C. difficile* was grown under anaerobic conditions at 37 °C in a Bactron III–2 chamber
88 (Shellab, OR, USA) in BHIS medium; 3.7% brain–heart infusion broth (BD, USA) supplemented
89 with 0.5% of yeast extract (BD, USA), and 0.1% L–cysteine (Merk, USA) liquid or on plates with
90 1.5% agar (BD, USA). *C. difficile* strain R20291 wild-type B1/NAP1/PCR-ribotype 027 strain
91 obtained from CRG0825 stock at Nottingham Clostridia Research Group (28). *C. difficile*

92 630Δ*erm* is a toxigenic (*tcdA*$^+$ *tcdB*$^+$) strain of *C. difficile* isolates from a patient with
93 pseudomembranous colitis during an outbreak of CDI (29). *C. difficile* 630Δ*erm bclA1::CT*,
94 630Δ*erm bclA2::CT* and 630Δ*erm bclA3::CT* are insertional inactivation clostron mutant strains
95 in the exosporium collagen-like proteins BclA1, BclA2 and BclA3 (30), and were a kind gift from
96 Dr. Simon Cutting (School of Biological Sciences, Royal Holloway, University of London).
97 *Bacillus megaterium* transformed with the plasmid pHIS 1622 that contains the cloned genes *tcdA*
98 and *tcdB* of *C. difficile* VPI 10463 (31), were aerobically grown at 37 °C in Luria-Bertani (BD)
99 with 10 µg/mL tetracycline.
100
101 **Cell lines and culture conditions**
102 Caco-2 cells (ATCC, USA) were grown at 37 °C with 5% CO_2 with Dulbecco's modified
103 Eagle's minimal essential medium High Glucose (DMEM; Hyclone, USA) supplemented with
104 10% of fetal bovine serum (FBS; Hyclone, USA) and 50 U mL^{-1} penicillin, and 50 µg mL^{-1}
105 streptomycin (Corning Cellgro, USA) as previously has been described For experiments, cells
106 were plated over glass coverslips in 24–well plates and were cultured for 2–days post–confluence
107 (undifferentiated) or 8–days post–confluence (differentiated), changing the media every other day.
108 To polarize Caco-2 cells were cultured onto 12mm Transwell (Corning, USA) with pores size of
109 0.4 µm until transepithelial electric resistance >250 Ω × cm^2.
110
111 **Recombinant *C. difficile* toxin Purification**
112 *C. difficile* toxins, TcdA and TcdB, were expressed in *B. megaterium* transformed with the
113 plasmid pHIS1622, containing the cloned genes *tcdA* and *tcdB* of *C. difficile* VPI 10463 as
114 previously described (31). Briefly, transformed *B. megaterium* were cultured in Luria–Bertani

115 medium (BD, USA) supplemented with 10 μg mL^{-1} tetracycline, and 35 mL of an overnight
116 culture was used to inoculate 1L of media. Bacteria were grown at 37 °C with 220 rpm. Toxin
117 expression was induced with 0.5% D–xylose once the culture reached OD_{600} = 0.5. Cells were
118 harvested after 4 h by centrifugation at 4,750×*g* and resuspended in 200 mL of binding buffer (20
119 mM Tris [pH 8.0], 100 mM NaCl for TcdA and 20 mM Tris [pH 8.0], 500 mM NaCl for TcdB)
120 supplemented with 0.16 μg mL^{-1} DNase, 10 mg mL^{-1} lysozyme and protease inhibitors (P8849;
121 Sigma). Cell lysis was performed using an Emulsiflex homogenizer, and lysates were centrifuged
122 at 48,000×*g* for 30 min. The toxins were purified from the supernatant by Nickel–affinity, anion
123 exchange, and size–exclusion chromatography. Toxins were eluted and stored in 20 mM HEPES
124 (pH 7.0), 50 mM NaCl.
125
126 **Spore preparation and purification**
127 *C. difficile* spores were purified as we previously described (32). Briefly, *C. difficile* spore
128 was cultured overnight in BHI medium in a Bactron III–2 anaerobic chamber (Shellab, USA).
129 Then a 1:500 dilution was plated in TY agar plates; 3% trypticase soy and 0.5% yeast extract and
130 1.5% Bacto agar (BD, USA) and incubated for 7 days at 37 °C in anaerobiosis. Colonies were
131 harvested with sterile, cold Milli–Q water, washed 3 times and purified with 50% Nicodenz. The
132 spore suspension was 99% free of vegetative cells, sporulating cells, and debris. Spores were
133 quantified in a Neubauer chamber and stored at –80 °C until use.
134
135 **Immunofluorescence of cell monolayers.**
136 To evaluate E-cadherin distribution in undifferentiated and differentiated Caco-2 cells,
137 cells were washed with PBS and were fixed with PBS–4% paraformaldehyde for 20 min at 4 °C,

138 blocked with PBS–3% BSA 1 h at room temperature (RT). To stain the accessible E-cadherin,
139 cells were incubated with 1: 50 of primary antibody mouse polyclonal anti–human E-cadherin (sc-
140 8426, Santa Cruz Biotechnology, USA) in PBS–3% BSA, for 2 h at RT followed by two washed
141 with PBS and 1:200 secondary antibody donkey anti–mouse-Alexa Fluor 568 (ab175700, Abcam,
142 USA). To detect the total E-cadherin, fixed samples were permeabilized with PBS-0.2% Triton
143 100-X for 10 min at RT and blocked with PBS–3% BSA for 1 h at RT. The total protein was
144 detected with the same primary antibody used accessible E-cadherin; primary antibody mouse
145 polyclonal anti–human E-cadherin (sc-8426, Santa Cruz Biotechnology, USA) in PBS–3% BSA
146 that was incubated for 2 h at RT, then were washed and was incubated with 1:200 secondary
147 antibody donkey anti–mouse-Alexa Fluor 568 (ab175700, Abcam, USA). The non–permeabilized
148 samples stained for accessible E-cadherin were permeabilized with PBS-0.2% Triton 100-X for
149 10 min at RT, washed, and to stain the F–actin, cells were incubated with 1:1,000 Phalloidin i–
150 Fluor 488 (ab176753, Abcam, USA) in PBS for 30 min at RT. Cells were washed, and nuclei were
151 stained with 8 μg mL^{-1} Hoechst 33342 (ThermoFisher, USA) in PBS for 10 min at RT. Then
152 samples were washed and mounted using Dako Fluorescent Mounting Medium (Dako, Denmark).
153 Samples were visualized in the confocal microscope Leica TCS LSI (Leica, Germany). Please see
154 below.
155
156 To study the redistribution of E-cadherin in TcdA/TcdB intoxicated cells, differentiated
157 Caco-2 cells cultured into 24–well plates were washed twice with DPBS (Hyclone, USA) and were
158 intoxicated with 600 pM TcdA and 600 pM TcdB for 3, 6, and 8 h in DMEM, without serum. As
159 a control, cells were incubated in the same solution without TcdA/TcdB. Then cells were rinsed
160 with PBS, fixed with PBS–4% paraformaldehyde, and washed with PBS and blocked with PBS–

161 1% BSA at 4 °C overnight. To stain the surface, accessible E-cadherin cells were incubated with
162 1:200 mouse mAb anti–E-cadherin (SC8426, Santa Cruz Biotechnologies, USA), 1 h at RT,
163 washed, and followed incubation with 1:400 donkey anti–mouse IgG Alexa Fluor 488 (ab150109,
164 Abcam, USA) for 1 h at RT. To detect the total protein, samples were permeabilized with PBS–
165 0.2% Triton 100-X for 10 min at RT and blocked with PBS–1% BSA for 1 h at RT. The total
166 protein was detected with the same primary antibody used before, washed, and samples were
167 incubated with donkey anti–mouse IgG Alexa Fluor 568 (ab175700, Abcam, USA). Samples were
168 mounted using Dako Fluorescent Mounting Medium (Dako, Denmark) and were visualized in the
169 confocal microscope Leica Sp8 (Leica, Germany; please see below.)
170
171 To evaluate *C. difficile* spore association with accessible E-cadherin in TcdA/TcdB intoxicated
172 IECs, differentiated Caco-2 cells were intoxicated with 600 pM TcdA and 600 pM TcdB for 8 h
173 at RT, as described above. Then cells were infected with *C. difficile* spores in an MOI of 10 for 1
174 h at 37 °C. Then cells were washed, fixed with PBS–4% paraformaldehyde for 10 min at RT,
175 blocked with PBS–1% BSA overnight at 4 °C, and *C. difficile* spores were stained with 1:1,000
176 primary polyclonal anti–*C. difficile* spore IgY batch 7246 antibodies (33) (Aveslab, USA) in PBS–
177 1% BSA for 1 h at RT. Following two PBS washed, samples were incubated with 1:400 goat anti–
178 chicken IgY secondary antibodies Alexa–Fluor 488 (#ab150173 Abcam, USA) in PBS–3% BSA
179 for 1 h at RT, washed two times with PBS, and accessible E–cadherin was stained as it is described
180 above. Cellular nuclei were stained with 8 μg mL^{-1} Hoechst 33342 (ThermoFisher, USA) for 15
181 min at RT. Finally, samples were mounted and analyzed by confocal microscopy Leica SP8.
182

183 The Leica microscopes TCS LSI and SP8 at the Confocal Microscopy Core Facility of the
184 Universidad Andrés Bello were used. To evaluate E-cadherin distribution in undifferentiated and
185 differentiated Caco-2 cells, Leica TCS LSI was used with 63× ACS APO oil objective numerical
186 aperture 1.3, with an optical zoom of 2×. Micrographs were acquired using excitation wavelengths
187 of 405, 488, and 532 nm, and signals were detected with an ultra–high dynamic photomultiplier
188 (PMT) spectral detector (430–750nm). Emitted fluorescence was split with four dichroic mirrors
189 (QD 405, 488, 561, and 635 nm). Images 1,024 × 1,024 pixels were acquired each 0.3 µm. To
190 observe the redistribution of accessible E-cadherin and total E-cadherin in TcdA and TcdB
191 intoxicated cells, Leica SP8 was used with HPL APO CS2 40× oil, numerical aperture 1.30. For
192 signal detection, three PMT spectral detectors were used; PMT1 (410–483) DAPI, PMT2 (505–
193 550), Alexa–Fluor 488, and PMT3 (587–726) Alexa–Fluor 555. Emitted fluorescence was split
194 with dichroic mirrors DD488/552. Pictures of 1,024 × 1,024 pixels were captured each 0.3 µm.
195 Images of 3–dimensional reconstructions of the Caco-2 monolayers were performed using ImageJ
196 software (NIH, USA). In undifferentiated and differentiated cells, accessible E-cadherin cells were
197 quantified as the number of cells with positives staining. To quantify the redistribution of E-
198 cadherin, Fl. Int. of each slide was measured using the plug–in "Measure stack" of Fiji (ImageJ,
199 NHI, USA), and the sum of the Fl. Int. of each slide is considered as the Fl. Int. of the *z*–stack of
200 a field for accessible and total E-cadherin. For each field, the same number of slides was used.
201

202 **Quantification of *C. difficile* spore adherence and internalization.**

203 To evaluate spore adherence and internalization in TcdA/TcdB intoxicated cells,
204 differentiated Caco-2 cells were incubated with 600 pM TcdA and 600 pM TcdB for 3, 6, and 8 h
205 in DMEM, without serum. As a control, cells were incubated in the same solution without

206 TcdA/TcdB or cells were incubated with TcdA/TcdB previously heat inactivated at 70°C for 5
207 min. Then cells were infected with *C. difficile* spores an MOI 10 for 3 h at 37 °C. Unbound spores
208 were rinsed off with PBS, and cells were fixed with PBS–4% paraformaldehyde for 10 min, and
209 adhered spores were stained as described below.
210
211 To evaluate spore adherence and entry in presence of anti–E-cadherin, undifferentiated,
212 differentiated, and polarized Caco-2 cells were incubated with 0,1; 1,0; 10; 100 µg mL^{-1} of mouse
213 monoclonal anti–human E-cadherin (SC8426, Santa Cruz Biotechnology, USA) or as control non–
214 immune IgG antibody of rabbit serum (I5006, Sigma-Aldrich, USA) for 2 h at 37 °C. Then cells
215 were infected for 3 h at 37 °C with *C. difficile* spores, previously incubated with 20 µL of FBS per
216 well for 1 h at 37 °C. Cells were washed two times with PBS to remove unbound spores and were
217 fixed with PBS–4% paraformaldehyde for 10 min at RT, and adhered spores were stained as
218 described below.
219
220 To evaluate spore adherence and entry in presence of purified E-cadherin, undifferentiated
221 and differentiated Caco-2 cells were infected with *C. difficile* spores previously incubated with 1,
222 2.5, 5, 10 and 25µg/mL of human purified E-cadherin (5085, Sigma-Aldrich, USA) in DMEM or
223 DMEM without FBS as control for 1 h at 37 °C. Then cells were infected and were incubated for
224 3 h at 37 °C. Cells were washed two times with PBS to remove unbound spores, fixed with PBS–
225 4% paraformaldehyde for 10 min at RT, and adhered spores were stained as described below.
226
227 To evaluate whether the presence of E-cadherin decreases the spore adherence in
228 TcdA/TcdB intoxicated cells, undifferentiated and differentiated Caco-2 cells were 8 h-

229 TcdA/TcdB intoxicated and were infected for 1 h at 37 °C with *C. difficile* spores previously
230 incubated with 25 µg/mL of E-cadherin for 1 h at 37 °C. Cells were washed two times with PBS
231 to remove unbound spores, fixed with PBS–4% paraformaldehyde for 10 min at RT, and adhered
232 spores were stained as described below.
233
234 In undifferentiated, differentiated, and polarized *C. difficile* spore infected Caco-2 cells,
235 adhered *C. difficile* spores were immunostained using the intracellular spore exclusion
236 immunostaining assay as previously described (20). For this *C. difficile* spore–infected cells were
237 washed three times with PBS at RT, blocked with PBS–3% BSA overnight at 4 °C, and samples
238 were incubated with anti–*C. difficile* spore goat serum 1:50 (PAC 5573, Pacific Immunology,
239 USA) in PBS–1% BSA for 1 h at RT. The cells were washed 3 times with PBS and incubated with
240 1:400 secondary antibody donkey IgG anti–goat CFL 488 (SC362255, Santa Cruz Biotechnology,
241 USA) for 1 h at RT. Cells were washed, and DNA was stained with 8 µg mL^{-1} Hoechst 33342
242 (ThermoFisher, USA) for 15 min at RT. In the case of polarized cells, to stain the F–actin, samples
243 were incubated with 1:100 Phalloidin Alexa Fluor 568 (A12380, Invitrogen, USA) for 30 min at
244 RT. Samples were washed three times with PBS and one time with distilled water and mounted
245 with Dako Fluorescent Mounting Medium (Dako, Denmark). Samples were visualized in the
246 epifluorescence microscope Olympus BX53 fluorescence microscopy with UPLFLN 100× oil
247 objective (numerical aperture 1.30). Images were captured with the camera for fluorescence
248 imaging Qimaging R6 Retiga, and pictures were analyzed with ImageJ (NIH, USA). Adhered
249 spores were considered as spores in phase–contrast that were marked in fluorescence. Internalized
250 spores were considered spores in phase–contrast, but that do not have fluorescence. In the case of

251 polarized cells, it was only possible to quantify adhered spores. The number or adhered spores
252 were quantified, and data were normalized to the control.
253
254 **ELISA of E-cadherin bound to *C. difficile* spores.**
255 Ninety six-well plate were coated overnight at 4ºC with 100 µL/well containing 1.6 x 10
256 *C. difficile* spores or 1 µg of BSA in PBS (as a control). overnight at 4 °C. Wells were washed 5
257 times with PBS–0.05% Tween-20 (PBS–Tween) to remove unbound spores and blocked with 200
258 µL of PBS–Tween–2% BSA (Sigma Aldrich, USA) for 1 h at 37 °C. The spores were washed and
259 incubated with 50 µL of 0.2, 2.0, 20, and 200 nM of recombinant human purified E-cadherin
260 (5085, Sigma-Aldrich, USA) for 1 h at 37 °C. Unbonded E-cadherin was washed 5 times with 150
261 µL PBS–Tween and was incubated with 50 µL of 1:50 IgG of mouse anti–E-cadherin (SC8426-
262 Santa Cruz Biotechnology, USA) in PBS–Tween–1% BSA for 1 h at 37 °C. Wells were washed
263 five times with PBS–Tween and then incubated with 50 µL of 1: 5,000 secondary antibody anti–
264 mouse-HRP (610-1302, Rockland, USA) 1 h at 37 °C. Then, wells were washed five times with
265 PBS–Tween and once with carbonate buffer (pH 9.6). Finally, wells were incubated with 50 µL
266 of buffer substrate (17 mM citric acid, 65 mM potassium phosphate, 0.15% hydrogen peroxide,
267 and 0.4% θ-phenylenediamine) for 20 min at RT. The reaction was stopped with 25 µL of 4.5 N
268 H_2SO_4. The color intensity was quantified at 450 nm using the plate reader Infinite F50, (Tecan,
269 Switzerland).
270
271 **Immunofluorescence of E-cadherin bound to *C. difficile* spores.**
272 The immunofluorescence was performed as previously described with modification (19).
273 Briefly, 4×10^7 *C. difficile* spores were incubated with 1, 2.5, 5.0, 10, and 25 µg mL^{-1} of

274 recombinant human purified E-cadherin (5085, Sigma-Aldrich, USA) in PBS for 1 h at 37 °C.
275 Spores were washed 5 times with PBS and fixed with PBS–4% paraformaldehyde in poly–L-
276 lysine-treated 12 mm glass–coverslips (Marienfeld GmbH, Germany). The spores were washed 3
277 times with PBS and were blocked with PBS–3% BSA for 1 h at RT. Then, samples were incubated
278 with 1:50 mouse IgG anti–E-cadherin (SC8426, Santa Cruz Biotechnology, USA) for 2 h at RT
279 and washed 3 times with PBS and once with distilled H_2O. Finally, samples were mounted with
280 Dako Fluorescent Mounting Medium (Dako, Denmark), and images were captured in an
281 epifluorescence microscope Olympus BX53. The fluorescence intensity was quantified using Fiji
282 (ImageJ, NHI, USA). Data were normalized as $(\text{Fl. Int/area})_{\text{sample}} - (\text{Fl. Int/area})_{\text{background}}$. The
283 Surface Plot was generated with the plug–in 3D surface Plot of Fiji (ImageJ, NHI, USA).
284
285 **SDS-PAGE and western blot of intoxicated Caco-2 cells.**
286 Undifferentiated and differentiated Caco-2 cells were intoxicated for 3, 6 and 8 h with TcdA/TcdB
287 in 24-well plates. The cells were washed and frozen at −80 °C. The frozen cells were lysed with
288 80 µL/well of cold RIPA buffer (50 mM Tris-HCl; 150 mM NaCl; 0.5% Deoxycholate; 1% NPO_4;
289 1mM EGTA; 1mM EDTA; 0.5% SDS; protease inhibitor) in ice and centrifuged at 18,400×*g* for
290 15 min at 4 °C. The supernatant was collected and 20 µg of protein was suspended in 2× SDS-
291 PAGE sample loading buffer, boiled and electrophoresed on 12% and 4% acrylamide SDS-PAGE
292 gels. Proteins were transferred to nitrocellulose membrane and blocked with 5% non-fat milk in
293 TBS for 1 h at RT. Membranes were probed for non-glucosylated Rac1 in Tris -buffered saline
294 containing 0.1% Tween (TTBS) with 5% milk and 1:1,000 mouse anti-Rac1 (Clone 102/Rac1
295 610650; BD Bioscience, USA) and then incubated overnight at RT and 6 h at RT. The membranes
296 were washed with TTBS and incubated with 1:5,000 goat anti-mouse HRP for 1 h at RT (Rockland

297 610-1302) in 5% milk-TTBS. Samples were washed 3 times with TTBS and HRP activity was
298 detected with a chemiluminescence detection system (Li-core) using PicoMax sensitive
299 chemiluminescence HRP substrate (Biorad, USA). To detect total Rac-1 in undifferentiated cells,
300 membranes were incubated twice with mild stripping solution (1.5% glycine, 0.1% SDS, 1%
301 Tween 20; pH 2.2) for 7 min at RT, washed twice with PBS and twice with TTBS 0.05%, and
302 blocked with 5% non-fat milk-TBS 1 h at RT. For differentiated cells, total Rac1 was detected in
303 the other membrane loaded simultaneously with the same concentration of protein. Membranes
304 were incubated with 1:1,000 mouse anti-Rac1 (clone 23A8 05-389; Merck Millipore, USA)
305 overnight at 4 °C and 3 h at RT and then washed 3 times with TTBS. Membranes were then
306 incubated with 1:5,000 goat anti-mouse HRP (Rockland 610-1302) 1 h at RT and washed 3 times
307 with TTBS. HRP activity was detected using Li-core as described for non-glucosylated Rac1.
308
309 **Transmission electron microscopy of E-cadherin bound to *C. difficile* spores.**
310 2.5×10^8 *C. difficile* spores were incubated with 10 µg mL^{-1} of recombinant human purified
311 E-cadherin (5085, Sigma-Aldrich, USA) with PBS for 1 h at 37 °C. Spores were washed 5 times
312 with PBS and centrifugation at 18,400×*g* for 5 min and were blocked with PBS–1% BSA for 20
313 min at RT. Then samples were incubated with 1:50 IgG of mouse anti–E-cadherin (SC8426, Santa
314 Cruz Biotechnologies, USA) in PBS–1% BSA for 1 h at RT, washed 3 times by centrifugation at
315 18,400×*g* for 5 min with PBS. Spores were incubated with IgG anti–mouse conjugated to 10nm
316 gold nanoparticles (G7777, Sigma-Aldrich, USA) for 1 h at RT. Then were washed 3 times with
317 PBS–0.1% BSA by centrifugation at 18,400×*g* for 5 min. Subsequently, spores were processes for
318 TEM, as previously have been described (19). Briefly, spores were fixed in 0.1 M cacodylate
319 buffer–2.5% glutaraldehyde with 1% paraformaldehyde and then fixed with 0.1 M cacodylate

320 buffer–1% osmium tetroxide and stained with 1% tannic acid for 30 min. Samples were dehydrated
321 with increasing acetone concentrations; 30% acetone (with 2% uranyl acetate only in this step) for
322 30 min, 50% acetone for 30 min, 70% acetone overnight, and 90% acetone for 30 min, and 2 times
323 with 100% acetone. Dehydrated samples were embedded in resin: acetone in a ratio of 3:1, 1:1,
324 and 1: 3 for 40 min each. Finally, samples were resuspended in resin for 4 h and incubated for 12
325 h at 65 °C. With a microtome, 90 nm sections cut and placed in a carbon–coated grid for negative
326 staining and double staining with 2% uranyl acetate with lead citrate. Sections were observed in a
327 transmission electron microscope Phillip Tecnai 12 bioTwin of the Pontificia Universidad Católica
328 de Chile. The distribution of thin or thick exosporium was quantified according to previously
329 described morphotypes (34).
330
331 **RESULTS**
332
333 **Characterization of accessible E-cadherin in monolayers of Caco-2 cells.** Caco-2 cells have
334 been employed to assess *C. difficile* interaction with IECs (18-20, 32, 33, 35-37). Early work
335 demonstrated that *C. difficile* spores had a tropism towards the cell-cell junction of EDTA-treated
336 Caco-2 cells (18). Therefore, to understand the dynamic of adherens junction closure during Caco-
337 2 cell differentiation, we assessed the accessibility of E-cadherin in undifferentiated and
338 differentiated monolayers of Caco-2 cells. First, Caco-2 cell differentiation was assessed for the
339 appearance of microvilli by TEM and sucrase-isomaltose as a differentiation marker in monolayers
340 cultured for 2- or 8-days post-confluency (19). Next, differentiated and undifferentiated Caco-2
341 cells were immunostained for accessible E-cadherin or permeabilized and stained for total E-
342 cadherin (Figure 1*A*, *B*). Results demonstrate that in undifferentiated Caco-2 cells, ~84% of the

343 cells were immunolabeled for accessible E-cadherin (Figure 1*C*), whereas, in differentiated Caco-
344 2 cells, only ~7% of the cells were stained for accessible E-cadherin (Figure 1*C*). As a control,
345 cells were permeabilized and stained for total E-cadherin, and we observed that ~100% of both
346 undifferentiated and differentiated Caco-2 cells were immunolabeled for E-cadherin (Figure 1*D-*
347 *F*). These results demonstrate that after 8-days of differentiation, most of the cells lack accessible
348 E-cadherin.
349
350 **Intoxication with *C. difficile* TcdA and TcdB increases accessible E-cadherin.** *C. difficile*
351 toxins TcdA and TcdB cause tight and adherens junction dissociation (9-11). TcdA, but not TcdB,
352 causes a displacement of E-cadherin from the cell-cell junctions to be located around the cells in
353 Caco-2 cells (11) while in colonic epithelium, TcdB causes adherens junctions disruption (10).
354 Since most of the *C. difficile* strains causing disease produces TcdA and TcdB (38), we asked
355 whether TcdA and TcdB affect the accessibility of E-cadherin in differentiated Caco-2 cells.
356 TcdA/TcdB-intoxicated differentiated Caco-2 cells for 3, 6, and 8 h were immunostained for
357 accessible E-cadherin (non-permeabilized) using an antibody that detects an extracellular domain
358 of E-cadherin, followed by fluorescent-labeled secondary antibody. For total E-cadherin staining,
359 cells were permeabilized and immunostained with the same primary antibody and a fluorescent-
360 labeled secondary antibody with another Alexa Fluor dye (See Methods). Then, we acquired
361 confocal micrographs, and the fluorescence intensity (Fl. Int.) was quantified for every slice of the
362 *z*-stack for accessible and total E-cadherin. The sum of the Fl. Int. of accessible E-cadherin was
363 significantly higher (175% relative to unintoxicated monolayers) after 8h-intoxication (Figure 2*A*,
364 *B*). To evaluate if this increase of Fl. Int. occurs in the apical or basal half of the monolayer, we
365 split the number of slices of the z-stack into 2-halves (apical and basal) with the same number of

366 slices. We summed the Fl. Int. for accessible E-cadherin in the apical (Figure 2*C*) or basal (Figure
367 2*D*) halves of the monolayer. We observed a significant increase in accessible E-cadherin Fl.Int.
368 in both the apical and basal halves, 177% and 176% respectively, after 8h-intoxication (Figure 2*C*,
369 *D*). Using the same strategy, we quantified the total E-cadherin Fl. Int. in the complete *z*-stack, and
370 we observed a significant decrease of 19% after 6h- and an increase of 12.2% after 8h-intoxication
371 compared to unintoxicated cells (Figure 2*E*). Then, we observed that these variations were in the
372 apical and not in the basal half of the monolayer. We observed a decrease of 35% after 6h- and an
373 increase of 44% after 8h-intoxication compared to unintoxicated cells (Figure 2*F*, *G*). To confirm
374 the degree of TcdA/TcdB intoxication, we evaluated the glucosyltransferase activity by measuring
375 the levels of glucosylated Rac1 in TcdA/TcdB intoxicated differentiated and undifferentiated
376 monolayers using strategies previously described (39). After 3 h of intoxication no modification
377 of Rac1 was observed. However, after 6 and 8 h of intoxication, the unglucosylated Rac1 signal
378 disappeared, indicating a complete glucosylation of Rac1 (Figure 2*H*). These results indicate that
379 the cells were fully intoxicated by 6 hours and accessible E-cadherin is increased in differentiated
380 Caco-2 cells after 8h-intoxication.
381
382 ***C. difficile* toxins TcdA and TcdB increase the adherence to IECs.** Several studies have shown
383 that vegetative *C. difficile*-adherence to IECs is enhanced following TcdA or CDT intoxication
384 (11, 40, 41). To expand the understanding of how intoxication of IECs impacts spore-adherence,
385 differentiated and undifferentiated Caco-2 cells were TcdA/TcdB intoxicated for 8 h, or incubated
386 8 h with heat inactivated TcdA/TcdB as a control. Then cells were washed and infected for 1 h
387 with *C. difficile* spores in the absence of serum. Cells were fixed and immunostained without
388 permeabilization. In TcdA/TcdB intoxicated Caco-2 cells, we observed more adhered spores

389 compared to unintoxicated cells (Figure 3*A*). After quantitative analysis, we observed in
390 undifferentiated Caco-2 cells that spore adherence in 8h-TcdA/TcdB-intoxicated cells was ~105%
391 higher than in unintoxicated monolayers, and no differences in spore adherence were observed in
392 cells 8 h-incubated with heat-inactivated TcdA/TcdB (Figure 3*B*). Similarly, in differentiated cells
393 we observed an increase in ~321% in 8 h-TcdA/TcdB-intoxicated cells over that in unintoxicated
394 monolayers, and no differences were observed in cells 8 h-incubated with heat-inactivated
395 TcdA/TcdB (Figure 3*C*). Collectively these data indicate that TcdA/TcdB intoxication of
396 undifferentiated and differentiated Caco-2 cells increases *C. difficile* spore adherence.
397
398 **Intoxication of IECs increases *C. difficile* spore association with E-cadherin.** Since we
399 observed that TcdA/TcdB-intoxicated differentiated Caco-2 cells lead to an increase of accessible
400 E-cadherin and adherence of *C. difficile* spores, we tested whether this could be attributed to *C.*
401 *difficile* spores associating with accessible E-cadherin. For this, unintoxicated or TcdA/TcdB-
402 intoxicated differentiated Caco-2 cells were infected with *C. difficile* spores for 1 h. Then,
403 accessible E-cadherin and spores were immunostained and visualized by confocal microscopy
404 (Figure 4*A*, *D*). Plot profile analysis of unintoxicated Caco-2 cells (Figure 4*A*) reveals that ~21%
405 of adhered *C. difficile* spores were associated with accessible E-cadherin (Figure 4*B, C,* and *G*).
406 Notably, upon TcdA/TcdB-intoxication (Figure 4*D*), ~72% of adhered spores were associated with
407 accessible E-cadherin (Figure 4*E*, *F, G*). These results indicate that adhered *C. difficile* spores can
408 associate with accessible E-cadherin in IECs, and this association is enhanced upon TcdA/TcdB-
409 intoxication.
410

411 **Antibody blocking of accessible E-cadherin reduces adherence and internalization of *C.***
412 ***difficile* spores to IECs.** Next, we assessed whether E-cadherin is involved in *C. difficile* spore
413 adherence and internalization. We have shown that *C. difficile* spore internalization occurs in the
414 presence of serum (20). Therefore, undifferentiated, differentiated, and polarized Caco-2 cells
415 were incubated with anti-E-cadherin antibody for 2h and subsequently infected for 3h with FBS-
416 incubated *C. difficile* spores. To identify intracellular spores, we used the intracellular spore
417 exclusion immunostaining assay (20), where only extracellular spores are immunostained in non-
418 permeabilized cells, and total spores are visualized by phase-contrast microscopy. Using this
419 strategy in undifferentiated Caco-2 cells, we observed that *C. difficile* spore adherence to IECs was
420 significantly decreased upon increasing concentrations of anti-E-cadherin antibody; spore
421 adherence decreased by 38, 53, and 73% compared to the control when cells were incubated with
422 1, 10, and 100 µg/mL of anti-E-cadherin antibody, respectively (Figure 5*A*). Upon quantifying
423 internalization in undifferentiated Caco-2 cells, we observed a significant decrease of 38, 43, and
424 69% compared to the control in cells incubated with 1, 10, 100 µg/mL of anti-E-cadherin,
425 respectively (Figure 5*B*). Similarly, in differentiated Caco-2 cells, a significant decrease in spore
426 adherence in 18, 32, 60, and 70% compared to the control was observed in cells incubated with
427 0.1, 1, 10, and 100 µg/mL of anti-E-cadherin, respectively (Figure 5*C*). For internalization, we
428 observed a significant decrease in 15, 35, 42, and 54% compared to the control in cells incubated
429 with 0.1, 1, 10, and 100 µg/mL of anti-E-cadherin, respectively (Figure 5*D*). Finally, in polarized
430 Caco-2 cells, we observed a decrease in 32, 56, 63, and 79% in spore adherence compared to the
431 control in presence with 0.1, 1, 10, and 100 µg/mL of anti-E-cadherin, respectively (Figure 5*E*).
432 These data indicate that the antibody-mediated blockage of accessible E-cadherin reduces *C.*
433 *difficile* spore adherence and internalization to IECs.

434

435 **Purified recombinant human E-cadherin competitively inhibits spore adherence in**
436 **undifferentiated, differentiated and TcdA/TcdB intoxicated IECs cells.** Subsequently, to
437 provide further evidence that E-cadherin acts as a spore adherence receptors, we evaluated whether
438 infected healthy undifferentiated Caco-2 monolayers with *C. difficile* spores preincubated with 1,
439 2.5, 5, 10, and 25 µg/mL of E-cadherin, and we observed a decrease in spore adherence of 12%,
440 26%, 38%, 47% and 64% respectively compared to spores not incubated with E-cadherin (Fig.
441 6*E*). In differentiated Caco-2 cells, we observed a decrease in spore adherence of 27%, 30%, 30%,
442 27% and 53% for spores incubated with 1, 2.5, 5, 10, and 25 µg/mL of E-cadherin, respectively
443 (Figure. 6*F*). Finally, we also assessed whether the increased spore adherence that we previously
444 observe in TcdA/TcdB intoxicated Caco-2 cells was E-cadherin specific. As expected, significant
445 *C. difficile* spore adherence to TcdA/TcdB intoxicated Caco-2 cells was observed in the absence
446 of E-cadherin; however, upon of TcdA/TcdB intoxicated differentiated and undifferentiated Caco-
447 2 cells with spores previously incubated with 25µg/mL of E-cadherin for 1 h at 37°C, and we
448 observed a significant decrease of 41% in undifferentiated (Figure 6*G*) and 55% in differentiated
449 Caco-2 cells (Figure 6*H*) compared to TcdA/TcdB intoxicated cells. Overall, these results show
450 that E-cadherin interacts with *C. difficile* spores in a dose-dependent manner and that E-cadherin-
451 ligand binding sites are non-homogeneously distributed on the *C. difficile* spore surface. There
452 results indicate that competition experiments with purified E-cadherin reduces the *C. difficile* spore
453 adherence in healthy and intoxicated cells.

454

455 **E-cadherin binds in a concentration-dependent manner to *C. difficile* spores.** To provide
456 evidence that *C. difficile* spores interact with E-cadherin, we used ELISA with *C. difficile* spore-

457 coated wells incubated with increasing concentrations of E-cadherin, or BSA as a control. E-
458 cadherin binding activity was evident in *C. difficile* spore-coated wells (Figure. 7*A*). The
459 specificity of this interaction was demonstrated by the dose-dependent binding. Additionally, we
460 evaluated the distribution of binding of E-cadherin to the spore surface by immunofluorescence.
461 Upon micrograph analysis, we observed that anti-E-cadherin immunostained spores exhibited a
462 non-homogeneous Fl. Int surrounding the spore (Figure. 7*B*). In spores, the Fl. Int. for E-cadherin
463 was 156, 189, 258, 304, and 369% relative to the control upon incubation with 1, 2.5, 5, 10, and
464 25 µg/mL of E-cadherin (Figure. 7*C*). Next, we established a Fl. Int cut-off limit for those *C.*
465 *difficile* spores that were visually associated with 2.5 µg/mL E-cadherin. Based on this threshold,
466 59, 65, and 66% of the spores were positive for E-cadherin in the presence of 5, 10, and 25 µg/mL
467 E-cadherin, respectively. Finally, we evaluated E-cadherin Fl. Int distribution for positive
468 immunodetected spores, and we observed that they were mainly distributed between 1.4-2.1
469 normalized Fl. Int. arbitrary units (Figure. 7*D*). Taken together, these results indicate that E-
470 cadherin binds in a concentration dependent manner to *C. difficile* spores, in a heterogeneous and
471 skewed manner to *C. difficile* spores.
472
473 **E-cadherin interacts with hair-like projections of *C. difficile* spores.** The outermost structure
474 of *C. difficile* spores are the hair-like projections, formed in part by BclA3, that are common in
475 epidemically relevant strains (16, 20, 42). Isogenic sporulating cultures of *C. difficile* lead to the
476 formation of spores with two exosporium morphotypes that exhibit hair-like projections, spores
477 with a thick exosporium layer display distinctive electron-dense bumps, and spores with a thin
478 exosporium lack these bumps (34, 42-44), suggesting that this exosporium morphotype diversity
479 might be contributing to E-cadherin spore-binding variability. Consequently, to gain ultrastructural

480 insight of the spore-E-cadherin interaction, *C. difficile* spores incubated with E-cadherin were
481 imaged by TEM and immunogold-labeling of E-cadherin. We observed E-cadherin-gold particles
482 in close contact with the exosporium of *C. difficile* spores, particularly with the hair-like
483 projections (Figure 8*A*-*E*). No gold particles were observed in spores without the E-cadherin
484 incubation. (Figure 8*A*). Next, within the E-cadherin positive spores, we observed gold particles
485 in 52/236 (22.1%) of the spores (Figure 8*F*). Of these, 19/52 (36.5%) and 33/52 (63.5%) of the E-
486 cadherin-bound spores corresponded to spores with thin and thick exosporiums, respectively
487 (Figure 8*G*). These results are representative of a 90 nm-slice of the sample, and therefore the
488 number of gold particles corresponds to those only present in the slice and not of a complete spore.
489 These results suggest that E-cadherin binds preferentially to thick-exosporium layer spores and
490 specifically to the hair-like projections.

491 Most *C. difficile* genomes encode three *bclA* orthologues encodes three collagen-like
492 proteins of the BclA family of proteins (45). However, *C. difficile* strain R20291 only encodes two *bclA*
493 orthologues (i.e., *bclA2* and *bclA3*) (45). Therefore, we reasoned to use previously characterized *bclA1*,
494 *bclA2* and *bclA3* mutants in strain 630 (30) to address by ELISA whether these collagen-like proteins could
495 be implicated in E-cadherin binding to *C. difficile* spores. As with R20291 spores, E-cadherin binding to
496 630 spore coated wells was evident (Figure 8E). Notably, upon coating wells with spores of *bclA1*,
497 *bclA2* or *bclA3* spores, a dose dependent binding of E-cadherin to spore-coated wells that as similar
498 to that of wild-type spores (Figure 8E). These results suggest the presence of an unidentified E-
499 cadherin-specific spore surface ligand.

500

501 **DISCUSSION**

502 A major clinical challenge that remains unresolved is how to address the high rates of CDI
503 recurrence (46-48). *C. difficile* spores are regarded as the key virulence factors required for

504 recurrence and transmission of the disease (16, 17). Although significant work has advanced our
505 understanding of the biology of *C. difficile* spores (16, 42), the mechanisms through which *C.*
506 *difficile* spores interact with the host within the environment of the colon remain poorly described.
507 The integrity of the intestinal epithelial barrier is key in preventing pathogen translocation (22).
508 However, in the healthy intestinal mucosa, the apical- and basolateral-cell sides are not always
509 separated. The adherens junctions, where E-cadherin is located, can be accessible in certain
510 situations, i.e., along lateral membranes of goblet cells (20, 49, 50), extruding apoptotic sites,
511 produced transiently when senescent cells are expelled and detached from the epithelium (49, 51,
512 52) and in epithelial folds of the intestinal villus produced by tension and constriction forces (49).
513 In this context, we have demonstrated that E-cadherin is a novel spore adherence-receptor that
514 promotes binding of *C. difficile* spores at adherens junctions, and this binding is enhanced in
515 intoxicated IECs.

516 Work by others have demonstrated that E-cadherin is hijacked by several pathogens,
517 including *Listeria monocytogenes*, *Fusobacterium nucleatum*, and *Streptococcus pneumoniae* (23-
518 26, 49). This report expands the list of pathogens that hijack E-cadherin for adherence and entry
519 to include *C. difficile* spores. Our prior work had demonstrated that *C. difficile* spores adhere to
520 IECs *in vitro* (18) and gain entry into host cells via fibronectin and vitronectin in an integrin-
521 dependent pathway (20). The ~70-80% reduction in adherence in undifferentiated, differentiated
522 and polarized monolayers of Caco-2 cells upon blockade with anti-E-cadherin antibodies or
523 competition with purified E-cadherin, suggests that E-cadherin is a major cellular adherence
524 receptor for *C. difficile* spores. Fibronectin, vitronectin, and integrin receptors are typically located
525 in the basolateral membrane (41, 53-56), where E-cadherin is localized. An outstanding question
526 is whether E-cadherin acts as an anchoring protein allowing *C. difficile* spores to bind

527 fibronectin/vitronectin and their cognate integrins to trigger internalization, or whether spore-
528 binding to E-cadherin alone is capable of triggering a signal for internalization of *C. difficile*
529 spores. This question will be addressed in future studies.
530
531 Another conclusion of this work is that *C. difficile* spores bind to E-cadherin in a dose-
532 dependent manner. *L. monocytogenes* interacts with human and not with mouse E-cadherin
533 through InlA (26). While the exosporium of *C. difficile* spores has no orthologs of InlA (57), we
534 show E-cadherin binding to the hair-like projections of the exosporium. Notably, spores of each
535 individual *bclA* orthologue in strain 630 were able to bind to E-cadherin to a similar extent as wild-
536 type spores, suggesting either redundance in function or the existence of an alternative spore
537 surface ligand(s) implicated in binding of E-cadherin to the spore surface. Current ongoing work
538 in our laboratory aims to identify the spore surface ligand(s) that bind to E-cadherin and its
539 implication in disease.
540
541 A final and major conclusion of this work is that TcdA/TcdB intoxication increases spore
542 adherence to IECs in a E-cadherin-specific manner. This is supported by increased association
543 between basolateral E-cadherin and *C. difficile* spores, and by the observation that soluble E-
544 cadherin can reduce the adherence of *C. difficile* spores to TcdA/TcdB intoxicated IECs. *C. difficile*
545 toxins TcdA and TcdB cause a disruption of the cell-cell junctions (10, 12, 13), causing a loss of
546 cellular polarity (9-11). This disruption is caused by a dissociation of tight and adherens junction
547 proteins. In this context, our work contributes to understanding how *C. difficile* spores interact
548 with TcdA/TcdB-intoxicated IECs. Our results demonstrate that differentiated TcdA/TcdB-
549 intoxicated monolayers show an increased accessibility of E-cadherin that correlates with an

550 increase in spore adherence to TcdA/TcdB-intoxicated cells. These observations suggest that
551 during CDI, TcdA and TcdB increase the E-cadherin accessibility, contributing to the spore
552 adherence and entry into the IECs *in vivo*. Indeed, since intracellular *C. difficile* spores contribute
553 to disease recurrence (20), TcdA/TcdB -intoxication may significantly contribute to *C. difficile*
554 spore adherence and internalization during CDI, contributing overall to disease recurrence. These
555 hypotheses are in agreement with clinical observations in CDI patients where high titers of
556 endogenous antibodies against the *C. difficile* toxins correlate with reduced R-CDI rates (58), and
557 with the reduced R-CDI observed in the clinical trials of bezlotoxumab (15). The development of
558 multifactorial treatment with intervention in TcdA/TcdB, spore adherence, and entry to IECs might
559 importantly reduce the R-CDI rates.
560

561 **NOTES**

562 ***CONFLICT OF INTEREST***. The authors declare that they have no conflict of interest.

563

564 ***FUNDING.*** This work was funded by FONDECYT Regular 1191601, and by Millennium Science

565 Initiative Program – NCN17_093, and Startup funds from the Department of Biology at Texas

566 A&M University to D.P-S. Additional funding support to P.C-C from ANID-PCHA/Doctorado

567 Nacional/ 2016-21161395.

568

569 **REFERENCES**

570

571 1. Redelings MD, Sorvillo F, Mascola L. 2007. Increase in *Clostridium difficile*-related
572 mortality rates, United States, 1999-2004. Emerg Infect Dis 13:1417-9.
573 2. Stevens VW, Nelson RE, Schwab-Daugherty EM, Khader K, Jones MM, Brown KA, Greene
574 T, Croft LD, Neuhauser M, Glassman P, Goetz MB, Samore MH, Rubin MA. 2017.
575 Comparative Effectiveness of Vancomycin and Metronidazole for the Prevention of
576 Recurrence and Death in Patients With *Clostridium difficile* Infection. JAMA Intern Med
577 177:546-553.
578 3. Di X, Bai N, Zhang X, Liu B, Ni W, Wang J, Wang K, Liang B, Liu Y, Wang R. 2015. A meta-
579 analysis of metronidazole and vancomycin for the treatment of *Clostridium difficile*
580 infection, stratified by disease severity. Braz J Infect Dis 19:339-49.
581 4. Lyerly DM, Lockwood DE, Richardson SH, Wilkins TD. 1982. Biological activities of toxins
582 A and B of *Clostridium difficile*. Infect Immun 35:1147-50.
583 5. Lyras D, O'Connor JR, Howarth PM, Sambol SP, Carter GP, Phumoonna T, Poon R, Adams
584 V, Vedantam G, Johnson S, Gerding DN, Rood JI. 2009. Toxin B is essential for virulence of
585 *Clostridium difficile*. Nature 458:1176-9.
586 6. Kuehne SA, Cartman ST, Heap JT, Kelly ML, Cockayne A, Minton NP. 2010. The role of toxin
587 A and toxin B in *Clostridium difficile* infection. Nature 467:711-3.
588 7. Just I, Selzer J, Wilm M, von Eichel-Streiber C, Mann M, Aktories K. 1995. Glucosylation of
589 Rho proteins by *Clostridium difficile* toxin B. Nature 375:500-3.
590 8. Just I, Wilm M, Selzer J, Rex G, von Eichel-Streiber C, Mann M, Aktories K. 1995. The
591 enterotoxin from *Clostridium difficile* (ToxA) monoglucosylates the Rho proteins. J Biol
592 Chem 270:13932-6.
593 9. Nusrat A, von Eichel-Streiber C, Turner JR, Verkade P, Madara JL, Parkos CA. 2001.
594 *Clostridium difficile* toxins disrupt epithelial barrier function by altering membrane
595 microdomain localization of tight junction proteins. Infect Immun 69:1329-36.
596 10. Mileto SJ, Jardé T, Childress KO, Jensen JL, Rogers AP, Kerr G, Hutton ML, Sheedlo MJ,
597 Bloch SC, Shupe JA, Horvay K, Flores T, Engel R, Wilkins S, McMurrick PJ, Lacy DB, Abud
598 HE, Lyras D. 2020. *Clostridioides difficile* infection damages colonic stem cells via TcdB,
599 impairing epithelial repair and recovery from disease. Proc Natl Acad Sci U S A 117:8064-
600 8073.
601 11. Kasendra M, Barrile R, Leuzzi R, Soriani M. 2014. *Clostridium difficile* toxins facilitate
602 bacterial colonization by modulating the fence and gate function of colonic epithelium. J
603 Infect Dis 209:1095-104.
604 12. Hecht G, Pothoulakis C, LaMont JT, Madara JL. 1988. *Clostridium difficile* toxin A perturbs
605 cytoskeletal structure and tight junction permeability of cultured human intestinal
606 epithelial monolayers. J Clin Invest 82:1516-24.
607 13. Hecht G, Koutsouris A, Pothoulakis C, LaMont JT, Madara JL. 1992. *Clostridium difficile*
608 toxin B disrupts the barrier function of T84 monolayers. Gastroenterology 102:416-23.

609 14. Leslie JL, Huang S, Opp JS, Nagy MS, Kobayashi M, Young VB, Spence JR. 2015. Persistence
610 and toxin production by *Clostridium difficile* within human intestinal organoids result in
611 disruption of epithelial paracellular barrier function. Infect Immun 83:138-45.
612 15. Wilcox MH, Gerding DN, Poxton IR, Kelly C, Nathan R, Birch T, Cornely OA, Rahav G, Bouza
613 E, Lee C, Jenkin G, Jensen W, Kim YS, Yoshida J, Gabryelski L, Pedley A, Eves K, Tipping R,
614 Guris D, Kartsonis N, Dorr MB, Investigators MIaMI. 2017. Bezlotoxumab for Prevention
615 of Recurrent *Clostridium difficile* Infection. N Engl J Med 376:305-317.
616 16. Paredes-Sabja D, Shen A, Sorg JA. 2014. *Clostridium difficile* spore biology: sporulation,
617 germination, and spore structural proteins. Trends Microbiol 22:406-16.
618 17. Deakin LJ, Clare S, Fagan RP, Dawson LF, Pickard DJ, West MR, Wren BW, Fairweather NF,
619 Dougan G, Lawley TD. 2012. The *Clostridium difficile spo0A* gene is a persistence and
620 transmission factor. Infect Immun 80:2704-11.
621 18. Paredes-Sabja D, Sarker MR. 2012. Adherence of *Clostridium difficile* spores to Caco-2
622 cells in culture. J Med Microbiol 61:1208-1218.
623 19. Mora-Uribe P, Miranda-Cardenas C, Castro-Cordova P, Gil F, Calderon I, Fuentes JA, Rodas
624 PI, Banawas S, Sarker MR, Paredes-Sabja D. 2016. Characterization of the Adherence of
625 *Clostridium difficile* Spores: The Integrity of the Outermost Layer Affects Adherence
626 Properties of Spores of the Epidemic Strain R20291 to Components of the Intestinal
627 Mucosa. Front Cell Infect Microbiol 6:99.
628 20. Castro-Córdova P, Mora-Uribe P, Reyes-Ramírez R, Cofré-Araneda G, Orozco-Aguilar J,
629 Brito-Silva C, Mendoza-León MJ, Kuehne SA, Minton NP, Pizarro-Guajardo M, Paredes-
630 Sabja D. 2021. Entry of spores into intestinal epithelial cells contributes to recurrence of
631 *Clostridioides difficile* infection. Nat Commun 12:1140.
632 21. Buckley A, Turner JR. 2018. Cell Biology of Tight Junction Barrier Regulation and Mucosal
633 Disease. Cold Spring Harb Perspect Biol 10.
634 22. Paradis T, Bègue H, Basmaciyan L, Dalle F, Bon F. 2021. Tight Junctions as a Key for
635 Pathogens Invasion in Intestinal Epithelial Cells. Int J Mol Sci 22.
636 23. Rubinstein MR, Wang X, Liu W, Hao Y, Cai G, Han YW. 2013. *Fusobacterium nucleatum*
637 promotes colorectal carcinogenesis by modulating E-cadherin/β-catenin signaling via its
638 FadA adhesin. Cell Host Microbe 14:195-206.
639 24. Anderton JM, Rajam G, Romero-Steiner S, Summer S, Kowalczyk AP, Carlone GM,
640 Sampson JS, Ades EW. 2007. E-cadherin is a receptor for the common protein
641 pneumococcal surface adhesin A (PsaA) of *Streptococcus pneumoniae*. Microb Pathog
642 42:225-36.
643 25. Elmi A, Nasher F, Jagatia H, Gundogdu O, Bajaj-Elliott M, Wren B, Dorrell N. 2016.
644 *Campylobacter jejuni* outer membrane vesicle-associated proteolytic activity promotes
645 bacterial invasion by mediating cleavage of intestinal epithelial cell E-cadherin and
646 occludin. Cell Microbiol 18:561-72.
647 26. Mengaud J, Ohayon H, Gounon P, Mege R-M, Cossart P. 1996. E-cadherin is the receptor
648 for internalin, a surface protein required for entry of *L. monocytogenes* into epithelial
649 cells. Cell 84:923-32.
650 27. Ribet D, Cossart P. 2015. How bacterial pathogens colonize their hosts and invade deeper
651 tissues. Microbes Infect 17:173-83.

652 28. Ng YK, Ehsaan M, Philip S, Collery MM, Janoir C, Collignon A, Cartman ST, Minton NP.
653 2013. Expanding the repertoire of gene tools for precise manipulation of the *Clostridium*
654 *difficile* genome: allelic exchange using *pyrE* alleles. PLoS One 8:e56051.
655 29. Wüst J, Sullivan NM, Hardegger U, Wilkins TD. 1982. Investigation of an outbreak of
656 antibiotic-associated colitis by various typing methods. J Clin Microbiol 16:1096-101.
657 30. Phetcharaburanin J, Hong HA, Colenutt C, Bianconi I, Sempere L, Permpoonpattana P,
658 Smith K, Dembek M, Tan S, Brisson MC, Brisson AR, Fairweather NF, Cutting SM. 2014.
659 The spore-associated protein BclA1 affects the susceptibility of animals to colonization
660 and infection by *Clostridium difficile*. Mol Microbiol 92:1025-38.
661 31. Chandrasekaran R, Kenworthy AK, Lacy DB. 2016. *Clostridium difficile* Toxin A Undergoes
662 Clathrin-Independent, PACSIN2-Dependent Endocytosis. PLoS Pathog 12:e1006070.
663 32. Calderon-Romero P, Castro-Cordova P, Reyes-Ramirez R, Milano-Cespedes M, Guerrero-
664 Araya E, Pizarro-Guajardo M, Olguin-Araneda V, Gil F, Paredes-Sabja D. 2018. *Clostridium*
665 *difficile* exosporium cysteine-rich proteins are essential for the morphogenesis of the
666 exosporium layer, spore resistance, and affect *C. difficile* pathogenesis. PLoS Pathog
667 14:e1007199.
668 33. Pizarro-Guajardo M, Diaz-Gonzalez F, Alvarez-Lobos M, Paredes-Sabja D. 2017.
669 Characterization of Chicken IgY Specific to *Clostridium difficile* R20291 Spores and the
670 Effect of Oral Administration in Mouse Models of Initiation and Recurrent Disease. Front
671 Cell Infect Microbiol 7:365.
672 34. Pizarro-Guajardo M, Calderon-Romero P, Castro-Cordova P, Mora-Uribe P, Paredes-Sabja
673 D. 2016. Ultrastructural Variability of the Exosporium Layer of *Clostridium difficile* Spores.
674 Appl Environ Microbiol 82:2202-2209.
675 35. Schöttelndreier D, Langejürgen A, Lindner R, Genth H. 2020. Low Density Lipoprotein
676 Receptor-Related Protein-1 (LRP1) Is Involved in the Uptake of *Clostridioides difficile* Toxin
677 A and Serves as an Internalizing Receptor. Front Cell Infect Microbiol 10:565465.
678 36. Tam J, Icho S, Utama E, Orrell KE, Gómez-Biagi RF, Theriot CM, Kroh HK, Rutherford SA,
679 Lacy DB, Melnyk RA. 2020. Intestinal bile acids directly modulate the structure and
680 function of *C.difficile* TcdB toxin. Proc Natl Acad Sci U S A 117:6792-6800.
681 37. Landenberger M, Nieland J, Roeder M, Nørgaard K, Papatheodorou P, Ernst K, Barth H.
682 2021. The cytotoxic effect of *Clostridioides difficile* pore-forming toxin CDTb. Biochim
683 Biophys Acta Biomembr 1863:183603.
684 38. Aktories K, Schwan C, Jank T. 2017. *Clostridium difficile* toxin biology. Annu Rev Microbiol
685 71:281-307.
686 39. Kroh HK, Chandrasekaran R, Zhang Z, Rosenthal K, Woods R, Jin X, Nyborg AC, Rainey GJ,
687 Warrener P, Melnyk RA, Spiller BW, Lacy DB. 2018. A neutralizing antibody that blocks
688 delivery of the enzymatic cargo of *Clostridium difficile* toxin TcdB into host cells. J Biol
689 Chem 293:941-952.
690 40. Schwan C, Stecher B, Tzivelekidis T, van Ham M, Rohde M, Hardt WD, Wehland J, Aktories
691 K. 2009. *Clostridium difficile* toxin CDT induces formation of microtubule-based
692 protrusions and increases adherence of bacteria. PLoS Pathog 5:e1000626.
693 41. Schwan C, Kruppke AS, Nolke T, Schumacher L, Koch-Nolte F, Kudryashev M, Stahlberg H,
694 Aktories K. 2014. *Clostridium difficile* toxin CDT hijacks microtubule organization and

695 reroutes vesicle traffic to increase pathogen adherence. Proc Natl Acad Sci U S A
696 111:2313-8.
697 42. Paredes-Sabja D, Cid-Rojas F, Pizarro-Guajardo M. 2022. Assembly of the exosporium
698 layer in Clostridioides difficile spores. Curr Opin Microbiol 67:102137.
699 43. Pizarro-Guajardo M, Calderon-Romero P, Paredes-Sabja D. 2016. Ultrastructure
700 Variability of the Exosporium Layer of *Clostridium difficile* Spores from Sporulating
701 Cultures and Biofilms. Appl Environ Microbiol 82:5892-8.
702 44. Pizarro-Guajardo M, Calderón-Romero P, Romero-Rodríguez A, Paredes-Sabja D. 2020.
703 Characterization of Exosporium Layer Variability of C*lostridioides difficile* Spores in the
704 Epidemically Relevant Strain R20291. Front Microbiol 11:1345.
705 45. Pizarro-Guajardo M, Olguin-Araneda V, Barra-Carrasco J, Brito-Silva C, Sarker MR,
706 Paredes-Sabja D. 2014. Characterization of the collagen-like exosporium protein, BclA1,
707 of *Clostridium difficile* spores. Anaerobe 25:18-30.
708 46. Lessa FC, Mu Y, Bamberg WM, Beldavs ZG, Dumyati GK, Dunn JR, Farley MM, Holzbauer
709 SM, Meek JI, Phipps EC, Wilson LE, Winston LG, Cohen JA, Limbago BM, Fridkin SK, Gerding
710 DN, McDonald LC. 2015. Burden of *Clostridium difficile* infection in the United States. N
711 Engl J Med 372:825-34.
712 47. Kelly CP. 2012. Can we identify patients at high risk of recurrent *Clostridium difficile*
713 infection? Clin Microbiol Infect 18:21-7.
714 48. Zhang S, Palazuelos-Munoz S, Balsells EM, Nair H, Chit A, Kyaw MH. 2016. Cost of hospital
715 management of Clostridium difficile infection in United States-a meta-analysis and
716 modelling study. BMC Infect Dis 16:447.
717 49. Nikitas G, Deschamps C, Disson O, Niault T, Cossart P, Lecuit M. 2011. Transcytosis of
718 *Listeria monocytogenes* across the intestinal barrier upon specific targeting of goblet cell
719 accessible E-cadherin. J Exp Med 208:2263-77.
720 50. Gessain G, Tsai YH, Travier L, Bonazzi M, Grayo S, Cossart P, Charlier C, Disson O, Lecuit
721 M. 2015. PI3-kinase activation is critical for host barrier permissiveness to *Listeria*
722 *monocytogenes*. J Exp Med 212:165-83.
723 51. Pentecost M, Otto G, Theriot JA, Amieva MR. 2006. *Listeria monocytogenes* invades the
724 epithelial junctions at sites of cell extrusion. PLoS Pathog 2:e3.
725 52. Pentecost M, Kumaran J, Ghosh P, Amieva MR. 2010. *Listeria monocytogenes* internalin B
726 activates junctional endocytosis to accelerate intestinal invasion. PLoS Pathog
727 6:e1000900.
728 53. Singh B, Su YC, Riesbeck K. 2010. Vitronectin in bacterial pathogenesis: a host protein used
729 in complement escape and cellular invasion. Mol Microbiol 78:545-60.
730 54. Henderson B, Nair S, Pallas J, Williams MA. 2011. Fibronectin: a multidomain host adhesin
731 targeted by bacterial fibronectin-binding proteins. FEMS Microbiol Rev 35:147-200.
732 55. Hamzaoui N, Kernéis S, Caliot E, Pringault E. 2004. Expression and distribution of beta1
733 integrins in in vitro-induced M cells: implications for *Yersinia* adhesion to Peyer's patch
734 epithelium. Cell Microbiol 6:817-28.
735 56. Clark MA, Hirst BH, Jepson MA. 1998. M-cell surface beta1 integrin expression and
736 invasin-mediated targeting of *Yersinia pseudotuberculosis* to mouse Peyer's patch M cells.
737 Infect Immun 66:1237-43.

738 57. Diaz-Gonzalez F, Milano M, Olguin-Araneda V, Pizarro-Cerda J, Castro-Cordova P, Tzeng
739 SC, Maier CS, Sarker MR, Paredes-Sabja D. 2015. Protein composition of the outermost
740 exosporium-like layer of *Clostridium difficile* 630 spores. J Proteomics 123:1-13.
741 58. Kelly CP, Poxton IR, Shen J, Wilcox MH, Gerding DN, Zhao X, Laterza OF, Railkar R, Guris
742 D, Dorr MB. 2020. Effect of Endogenous *Clostridioides difficile* Toxin Antibodies on
743 Recurrence of *C. difficile* Infection. Clin Infect Dis 71:81-86.
744

745

746

747

748 **Figure Legends**

749 **Figure 1. Distribution of accessible and total E-cadherin in undifferentiated and**
750 **differentiated Caco-2 cells.** 3D projection of a representative confocal micrograph of healthy *A*,
751 undifferentiated, and *B*, differentiated Caco-2 cells immunostaining for accessible E-cadherin.
752 Accessible E-cadherin (shown as acc Ecad) is in green, F-actin in red, and nuclei in blue. *C*,
753 Repartition of cells that were positive (Ecad+) or negative (Ecad−) stained for accessible E-
754 cadherin. 3D projection of a representative confocal micrograph of a healthy *D*, undifferentiated
755 and *E*, differentiated Caco-2 cells immunostaining for total E-cadherin and *F*, Repartition of cells
756 that were positive (Ecad+) or negative (Ecad−) stained for total E-cadherin. Fluorophores colors
757 were digitally reassigned for a better representation. Micrographs are representative of 6 fields of
758 2 independent experiments. Scale bar, 20µm. Error bars indicate mean ± SEM. Statistical analysis
759 was performed by two-tailed unpaired Student's *t*-test, ns, $p > 0.05$; ****, $p \leq 0.0001$.

760

761 **Figure 2. The accessibility of E-cadherin increases in TcdA and TcdB intoxicated IECs.**
762 Differentiated TcdA/TcdB intoxicated Caco-2 cells for 3, 6, or 8 h in DMEM without serum. As a
763 control, cells were incubated with DMEM without serum. Non-permeabilized cells were stained
764 for accessible E-cadherin (shown as acc Ecad; green), permeabilized, and total E-cadherin was
765 stained (shown as total Ecad; red) and nuclei (blue). *A*, Representative confocal microscopy images
766 3D (XY) projection of control cells (left) and TcdA/TcdB intoxicated cells for 8h (right); below
767 the orthogonal view (XZ; accessible E-cadherin, total E-cadherin and merged) of the dotted line
768 of the XY. Representative confocal images for 3h and 8h not shown. Relative Fl. Int. measured as
769 the sum of each z-step of *B*, accessible E-cadherin, and its abundance in the *C*, apical side, or *D* in
770 the basal side of the cell. Relative Fl.Int. of *E*, total E-cadherin, its abundance in the *F*, apical side,

771 and the *G*, basal side of the cell. Controls were set 100%. Error bars indicate the mean ± SEM
772 from at least 9 fields ($n = 3$). *H*, immunoblotting anti non-glucosylated Rac1 and total Rac1 of cell
773 lysates of undifferentiated and differentiated Caco-2 cells intoxicated with TcdA/TcdB for 3, 6 or
774 8h. For undifferentiated in non-glucosylated Rac1 was evaluated, then stripped and membranes
775 were tested for total Rac1. Meanwhile for differentiated cells, the same sample was solved in 2
776 independent membranes simultaneously and were independently tested for non-glucosylated and
777 total Rac1. Western blot are representative of 3 independent experiment. Statistical analysis was
778 performed by two-tailed unpaired Student's *t*-test, ns, $p > 0.05$; ****, $p < 0.0001$. Bars, 5µm.
779

780 **Figure 3. TcdA and TcdB increase *C. difficile* spore interaction with IECs.**

781 Differentiated TcdA/TcdB intoxicated Caco-2 cells for 8h or incubated with DMEM without
782 serum as control and then, were washed with PBS and infected for 3h at an MOI 10 with *C. difficile*
783 spores. Unbound spores were rinsed off. Non-permeabilized cells were stained for adhered spores.
784 *A*, Representative epifluorescence microscopy images of TcdA and TcdB intoxicated cells (or
785 DMEM as control) for 8h then washed and infected with *C. difficile* spore. *B*, *C. difficile* spore
786 adherence relative in *B*, undifferentiated and *C*, differentiated cells. In bars, each dot represents
787 one independent well from 2 independent experiment, Per each well a total of 5 fields were
788 analyzed. Error bars indicate the mean ± SEM.. Statistical analysis was performed by unpaired *t*-
789 test, ns, $p > 0.05$. Bars, 10 µm.
790

791 **Figure 4. E-cadherin of IECs interacts with *C. difficile* spores increasing in TcdA and TcdB**
792 **intoxicated cells.**

793 Differentiated Caco-2 cells were intoxicated with TcdA and TcdB for 8 h at 37 °C in DMEM

794 without serum. As a control, cells were incubated with DMEM without serum. Then cells were
795 infected with *C. difficile* spores for 1 h at 37 °C. Non-permeabilized cells were stained for
796 accessible E-cadherin (shown as acc Ecad; green), spores (red), and nuclei (blue). *A*,
797 Representative 3D projection confocal micrograph of healthy cells infected with *C. difficile* spores
798 (Ctrl). On the right, magnifications of representative *C. difficile* spores associated or not with E-
799 cadherin. *B*, *C,* Plot profile Fl.Int. of *C. difficile* spores (red line) and accessible E-cadherin (shown
800 as Ecad, green line) performed in the white line of *A*. *D*, Representative 3D projection confocal
801 micrograph of TcdA and TcdB intoxicated cells infected with *C. difficile* spores. On the right
802 magnifications of representative *C. difficile* spores associated or not with E-cadherin. *E, F*, Plot
803 profile Fl.Int. of *C. difficile* spores (red) and accessible E-cadherin (shown as Ecad, in green)
804 performed in the white line of *D*. Repartition of spores that were positive (Ecad+) or negative
805 (Ecad−) associated with fluorescence signal for accessible E-cadherin was shown as the average
806 associated/non-associated spores with E-cadherin for each field, a total of ~500 spores were
807 analyzed. Fluorophores were digitally reassigned for a better representation. Micrographs are
808 representative of 6 independent fields of 3 different experiments. Error bars indicate mean ± SEM.
809 Statistical analysis was performed by two-tailed unpaired Student's *t*-test, ns, $p > 0.05$; **, $p \leq$
810 0.01; ***, $p \leq 0.001$. Bars, 10μm.
811
812 **Figure 5. E-cadherin blocking antibodies decrease the spore interaction with IECs.**
813 Undifferentiated, differentiated, and polarized Caco-2 cells were infected with *C. difficile* spores
814 preincubated with FBS in the presence of anti-E-cadherin or non-immune IgG as control for 2 h at
815 37 °C. *A*, adherence, and *B*, internalization of *C. difficile* spores in undifferentiated Caco-2 cells
816 or *C*, adherence and *D*, internalization in differentiated Caco-2. *E, C. difficile* spore adherence in

817 polarized Caco-2 cells. Data showed in each panel are normalized to 0 µg mL^{-1} of antibody.
818 The data are the mean of 6 independent wells collected in 2 independent experiments. In bars, each
819 dot represents one independent well collected from 2 independent experiments. For each bar, a
820 total of ~1,300 spores were analyzed. Error bars indicate mean ± SEM. Statistical analysis was
821 performed by two-tailed unpaired Student's *t*-test, ns, $p > 0.05$; ****, $p < 0.0001$.
822
823 **Figure 6. E-cadherin competitively reduces spore adherence to healthy and intoxicated**
824 **IECs.**
825 *A* Undifferentiated and differentiated Caco-2 cells where infected for 3 h at a MOI of 10 with *C.*
826 *difficile* spores pretreated with 1, 2.5, 5, 10 and 25µg/mL of human purified E-cadherin, and
827 adhered cells where identified and quantified as described in the Method section. *B*. TcdA/TcdB
828 intoxicated undifferentiated and differentiated Caco-2 cells where infected for 3 h at a MOI of 10
829 with *C. difficile* spores pretreated with 25µg/mL of human purified E-cadherin, and adhered cells
830 where identified and quantified as described in the Method section. The data are the mean of 6
831 independent wells collected in 2 independent experiments. Adherence of *C. difficile* spores
832 preincubated with E-cadherin (or DMEM as control) in 8 h-TcdA/TcdB intoxicated cells. The
833 data are the mean of 6 independent wells collected in 2 independent experiments.
834
835 **Figure 7. E-cadherin interacts with *C. difficile* spore.**
836 *A*, Solid-phase binding assay of *C. difficile* R20291 spores or BSA as control with increasing
837 concentrations (i.e., 0.2, 2.0, 20 and 200 nM) of human purified E-cadherin. The data represented
838 are the mean of 9 independent wells collected in 3 independent experiments. *B*, Representative
839 phase-contrast micrograph, immunofluorescence against E-cadherin, and immunofluorescence

840 plot profile of 4×10^7 *C. difficile* spores that were incubated with increasing concentrations (i.e.,
841 1, 2.5, 5, 10, 25 μg mL^{-1}) of human purified E-cadherin for 1 h at 37 °C. *C*, Quantitative analysis
842 of Fl.Int. *D*, Distribution of E-cadherin fluorescence intensity of *C. difficile* incubated with
843 increasing concentrations (i.e., 1, 2.5, 5, 10, 25 μg mL^{-1}) of human purified E-cadherin. A total of
844 ~450 spores were analyzed for each condition. Error bars indicate mean ± SEM. Statistical analysis
845 was performed by two-tailed unpaired Student's *t*-test, ns, $p > 0.05$; *, $p < 0.05$; ****, $p < 0.0001$.
846

847 **Figure 8. Immunoelectron microscopy of E-cadherin-gold complex binds to *C. difficile***
848 **spores.**

849 *A*,*B* TEM of *C. difficile* spores incubated with 10 μg mL^{-1} E-cadherin or without E-cadherin
850 (negative control). Then incubated with anti-E-cadherin and anti-mouse-gold 12 nm complex.
851 White arrows denote the mouse anti-E-cadherin and anti-mouse-gold 12 nm complex. Spores
852 where stratified in thick and thin exosporium spores. Lower panels are magnification of the black
853 squares highlighting immunogold spots, Quantification of the *C. difficile* spore associated with E-
854 cadherin ("−" and "+" denote negative or positive association, respectively). *C,D* Classification of
855 E-cadherin positively associated *C. difficile* spores according to the morphology of the spore, thin
856 or thick exosporium, represented as the percentage of the total E-cadherin positive spores. Figures
857 show representative spores with a thin or thick exosporium layer, and are representative of 2
858 independent experiments. A total of 100 spores were quantified. *E* solid-phase binding assay of
859 human E-cadherin to *C. difficile* spores of 630 wild-type and isogenic mutant strains of *bclA1*,
860 *bclA2* and *bclA3* or BSA as a control with increasing concentrations (i.e., 0.2, 2.0, 20 and 200 nM)
861 of human purified E-cadherin. The data represented are the mean of 9 independent wells collected
862 in 3 independent experiments.

863

864

865 **Supplementary figures review only.**

866

867 **Supplementary confocal micrographs of Fig. 1.**

868 These are supplementary figures from the experiment detailed in Fig. 4. Differentiated Caco-2
869 cells intoxicated with 600 pM of TcdA and TcdB for 3, 6, or 8 h in DMEM without serum. As a
870 control, cells were treated with DMEM without serum. Non-permeabilized cells were stained for
871 accessible E-cadherin (shown as acc Ecad) in green, then permeabilized and stained total E-
872 cadherin (total Ecad) shown in red nuclei shown in blue. Representative confocal microscopy
873 images 3D (XY) projection of intoxicated cells for 3 h (left) or 6 h (right) with its control; below
874 a magnified slide (XY), and the orthogonal view (XZ). Representative images from at 9 fields (*n*
875 = 3). Bars, 5μm.

876

877

Figure 1

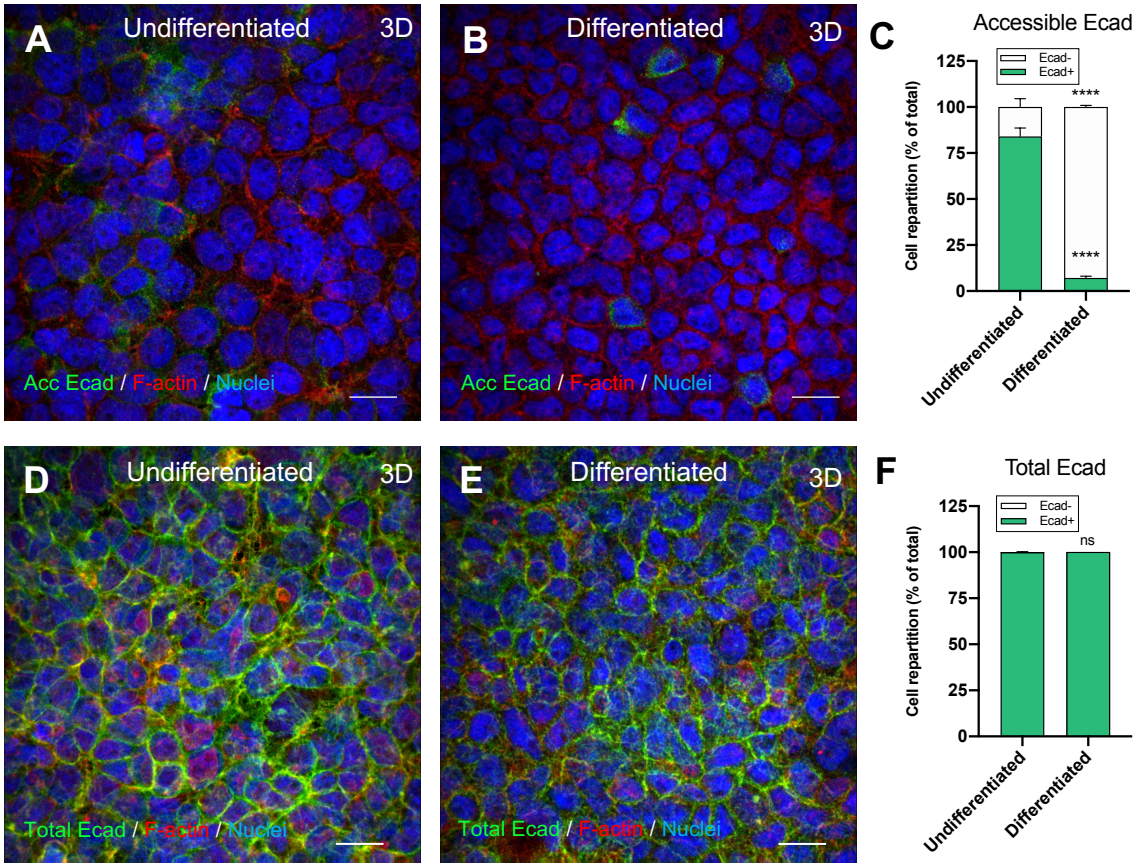
A
Undifferentiated
3D
Acc Ecad / F-actin / Nuclei
B
Differentiated
3D
Acc Ecad / F-actin / Nuclei
C
Accessible Ecad
Ecad-
Ecad+
Cell repartition (% of total)
125
100
75
50
25
0
****
****
Undifferentiated
Differentiated
D
Undifferentiated
3D
Total Ecad / F-actin / Nuclei
E
Differentiated
3D
Total Ecad / F-actin / Nuclei
F
Total Ecad
Ecad-
Ecad+
Cell repartition (% of total)
125
100
75
50
25
0
ns
Undifferentiated
Differentiated

Figure 2

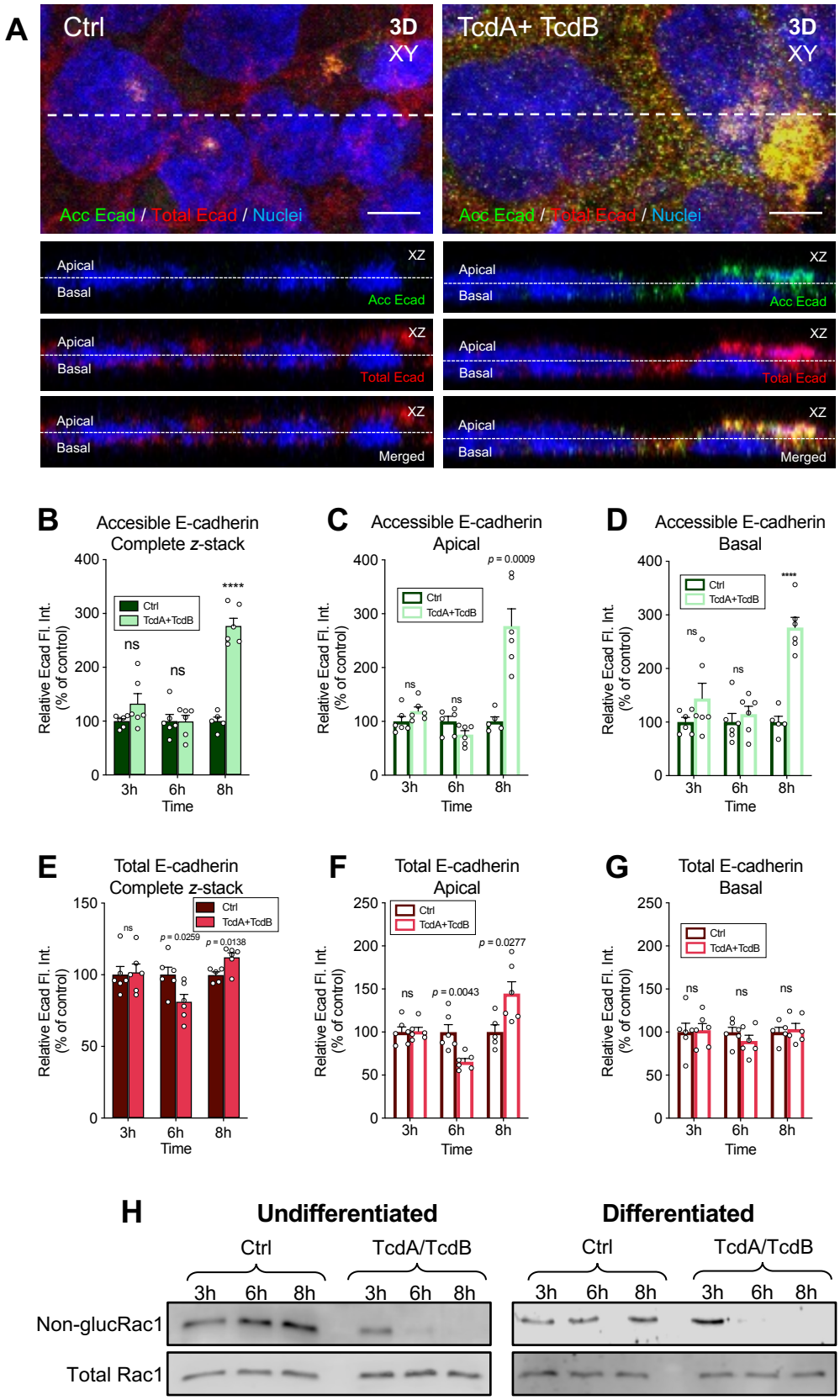
A
Ctrl
3D
XY
Acc Ecad / Total Ecad / Nuclei
TcdA+ TcdB
Apical
Basal
XZ
Acc Ecad
Total Ecad
Merged
B
Accesible E-cadherin
Complete z-stack
C
Accessible E-cadherin
Apical
D
Accessible E-cadherin
Basal
E
Total E-cadherin
Complete z-stack
F
Total E-cadherin
Apical
G
Total E-cadherin
Basal
Relative Ecad Fl. Int.
(% of control)
Ctrl
TcdA+TcdB
ns
p = 0.0009
p = 0.0259
p = 0.0138
p = 0.0043
p = 0.0277
3h
6h
8h
Time
H
Undifferentiated
Differentiated
Ctrl
TcdA/TcdB
Non-glucRac1
Total Rac1

Figure 3

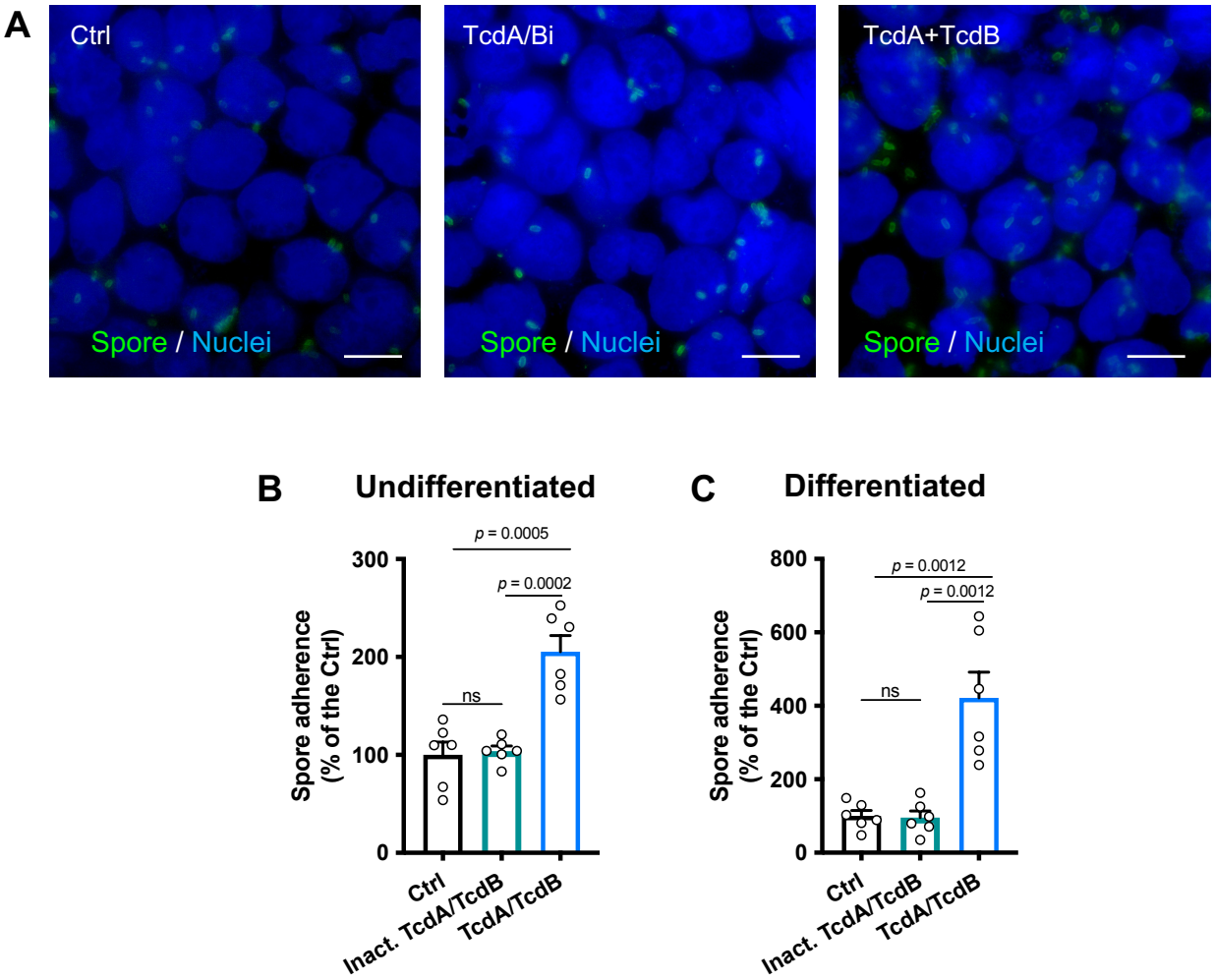
A
Ctrl
Spore / Nuclei
TcdA/Bi
Spore / Nuclei
TcdA+TcdB
Spore / Nuclei
B
Undifferentiated
Spore adherence (% of the Ctrl)
300
200
100
0
p = 0.0005
p = 0.0002
ns
Ctrl
Inact. TcdA/TcdB
TcdA/TcdB
C
Differentiated
Spore adherence (% of the Ctrl)
800
600
400
200
0
p = 0.0012
p = 0.0012
ns
Ctrl
Inact. TcdA/TcdB
TcdA/TcdB

Figure 4

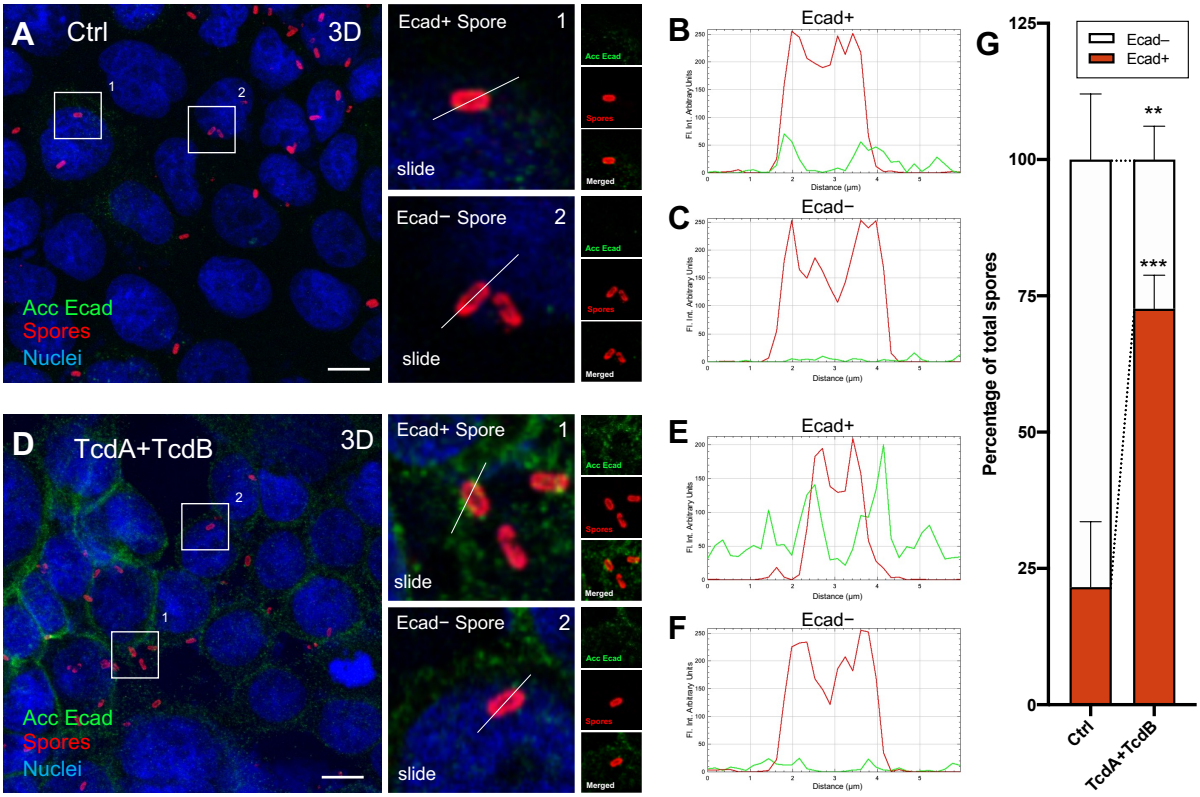
A
Ctrl
3D
1
2
Acc Ecad
Spores
Nuclei
Ecad+ Spore
1
slide
Ecad− Spore
2
slide
Acc Ecad
Spores
Merged
B
Ecad+
C
Ecad−
E
Ecad+
F
Ecad−
Fl. Int. Arbitrary Units
Distance (µm)
D
TcdA+TcdB
3D
1
2
Acc Ecad
Spores
Nuclei
Ecad+ Spore
1
slide
Ecad− Spore
2
slide
Acc Ecad
Spores
Merged
G
Ecad−
Ecad+
Percentage of total spores
125
100
75
50
25
0
**
***
Ctrl
TcdA+TcdB

Figure 5

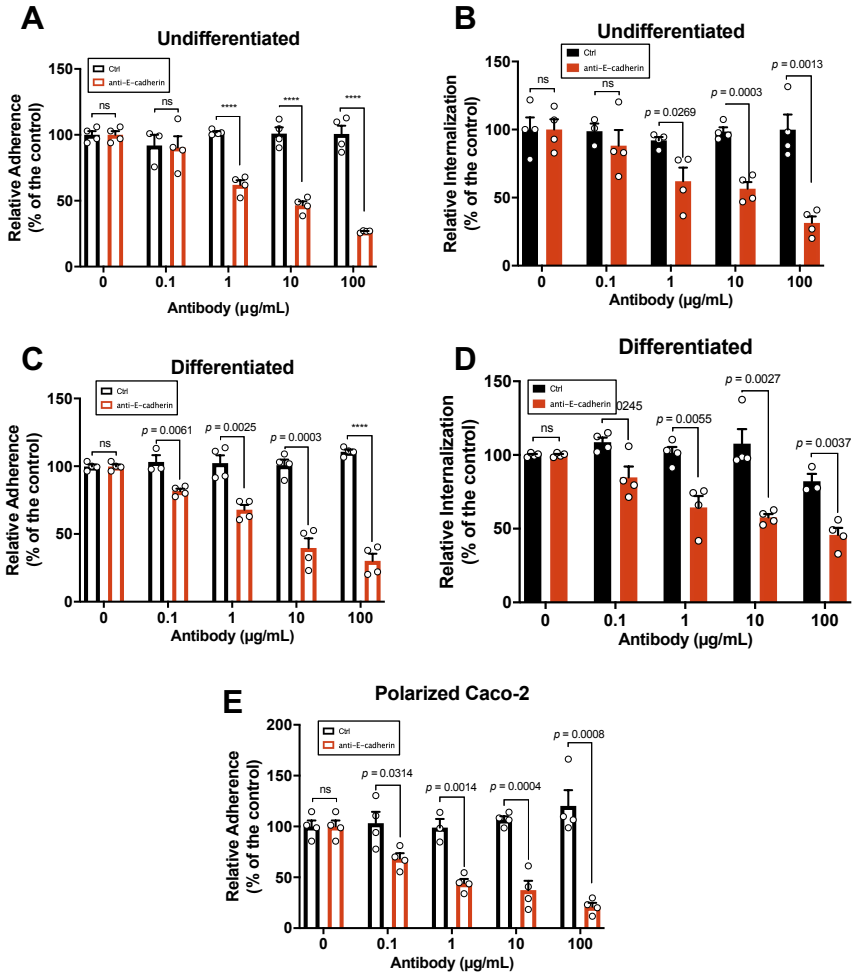
A
Undifferentiated
Ctrl
anti-E-cadherin
Relative Adherence (% of the control)
ns
ns
****
****
****
Antibody (µg/mL)
B
Undifferentiated
Relative Internalization (% of the control)
ns
ns
p = 0.0269
p = 0.0003
p = 0.0013
C
Differentiated
p = 0.0061
p = 0.0025
p = 0.0003
D
Differentiated
p = 0.0245
p = 0.0055
p = 0.0027
p = 0.0037
E
Polarized Caco-2
p = 0.0314
p = 0.0014
p = 0.0004
p = 0.0008

Figure 6

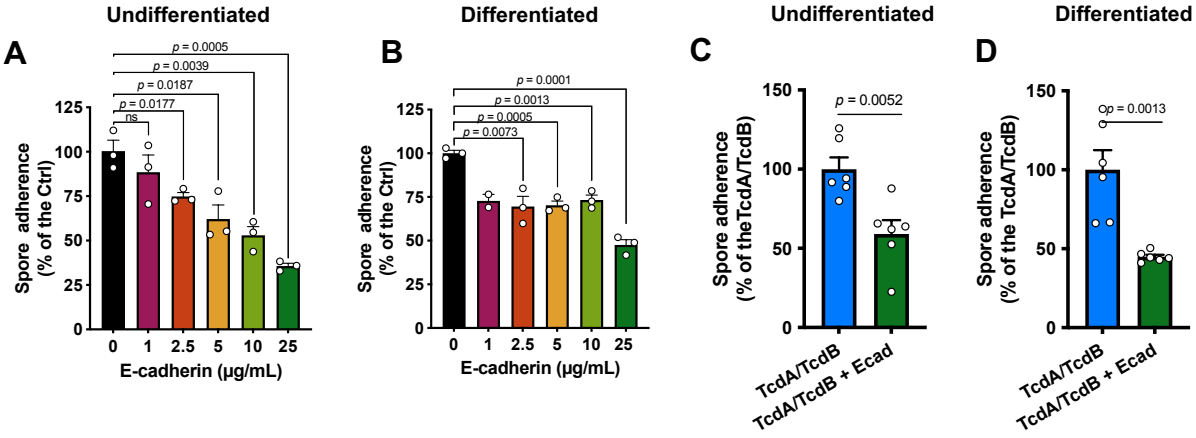
Undifferentiated
A
p = 0.0005
p = 0.0039
p = 0.0187
p = 0.0177
ns
Spore adherence (% of the Ctrl)
125
100
75
50
25
0
0
1
2.5
5
10
25
E-cadherin (µg/mL)
Differentiated
B
p = 0.0001
p = 0.0013
p = 0.0005
p = 0.0073
Spore adherence (% of the Ctrl)
E-cadherin (µg/mL)
Undifferentiated
C
p = 0.0052
Spore adherence (% of the TcdA/TcdB)
150
100
50
0
TcdA/TcdB
TcdA/TcdB + Ecad
Differentiated
D
p = 0.0013
Spore adherence (% of the TcdA/TcdB)
TcdA/TcdB
TcdA/TcdB + Ecad

Figure 7

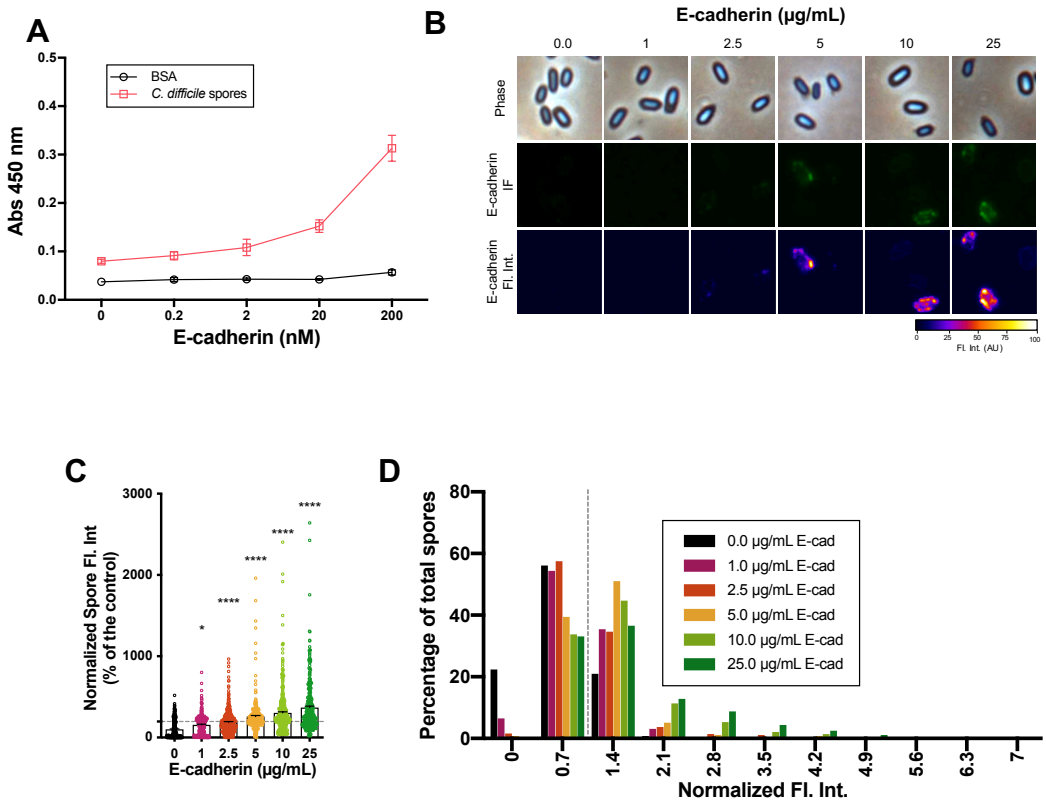
A
BSA
C. difficile spores
Abs 450 nm
E-cadherin (nM)
B
E-cadherin (µg/mL)
Phase
E-cadherin IF
E-cadherin Fl. Int.
Fl. Int. (AU)
C
Normalized Spore Fl. Int (% of the control)
E-cadherin (µg/mL)
D
Percentage of total spores
0.0 µg/mL E-cad
1.0 µg/mL E-cad
2.5 µg/mL E-cad
5.0 µg/mL E-cad
10.0 µg/mL E-cad
25.0 µg/mL E-cad
Normalized Fl. Int.

Figure 8

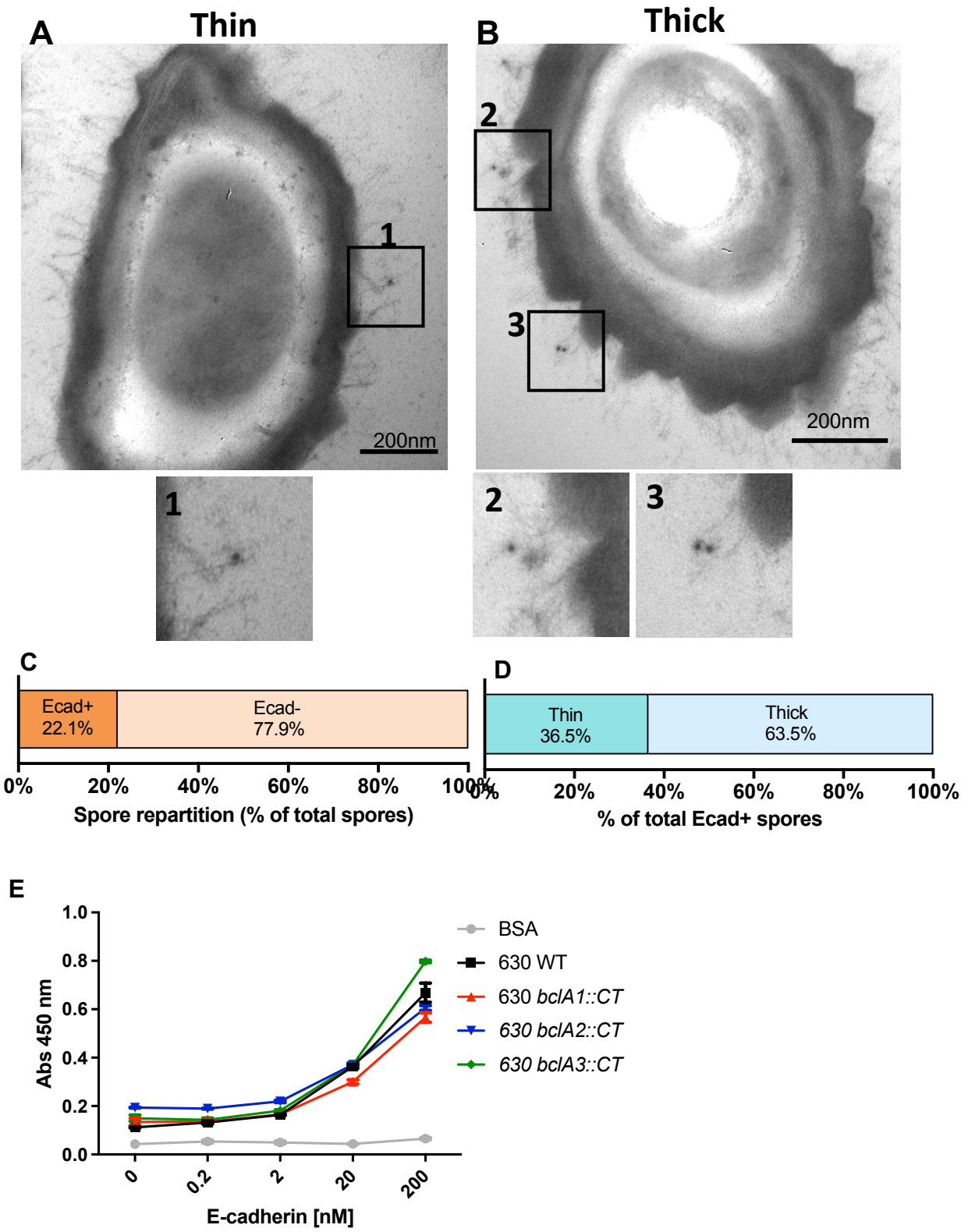
A
Thin
1
200nm
1
B
Thick
2
3
200nm
2
3
C
Ecad+
22.1%
Ecad-
77.9%
0%
20%
40%
60%
80%
100%
Spore repartition (% of total spores)
D
Thin
36.5%
Thick
63.5%
0%
20%
40%
60%
80%
100%
% of total Ecad+ spores
E
Abs 450 nm
1.0
0.8
0.6
0.4
0.2
0.0
0
0.2
2
20
200
E-cadherin [nM]
BSA
630 WT
630 bclA1::CT
630 bclA2::CT
630 bclA3::CT
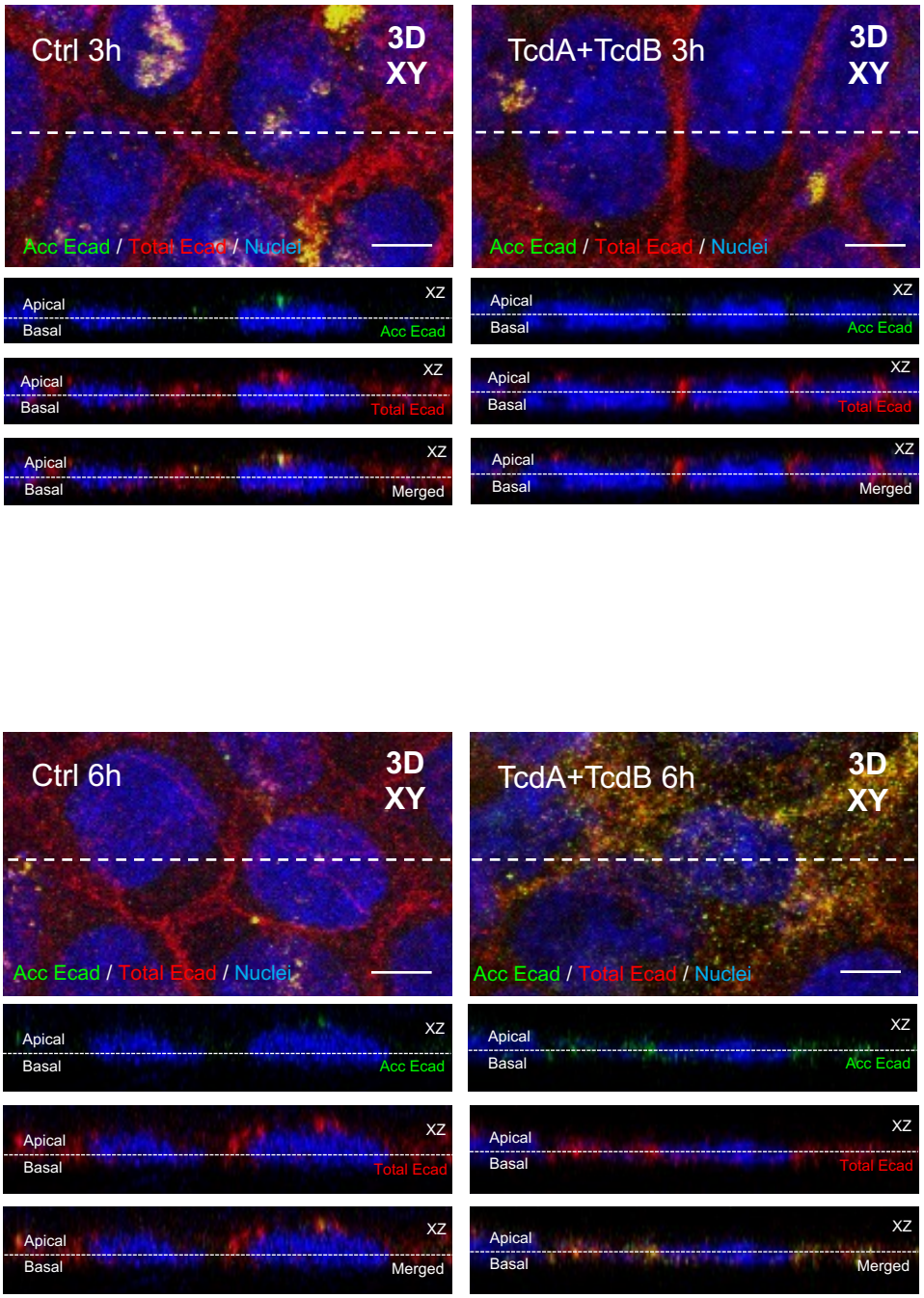
Supplementary Fig 1